3228–3245 *Nucleic Acids Research, 2014, Vol. 42, No. 5* *Published online 25 December 2013*
doi:10.1093/nar/gkt1321

Inhibition of translation by IFIT family members is determined by their ability to interact selectively with the 5′-terminal regions of cap0-, cap1- and 5′ppp- mRNAs

Parimal Kumar†, Trevor R. Sweeney†, Maxim A. Skabkin, Olga V. Skabkina, Christopher U.T. Hellen and Tatyana V. Pestova*

Department of Cell Biology, SUNY Downstate Medical Center, 450 Clarkson Avenue, Brooklyn, NY 11203, USA

Received November 1, 2013; Revised November 22, 2013; Accepted November 27, 2013

ABSTRACT

Ribosomal recruitment of cellular mRNAs depends on binding of eIF4F to the mRNA's 5′-terminal 'cap'. The minimal 'cap0' consists of N7-methylguanosine linked to the first nucleotide via a 5′-5′ triphosphate (ppp) bridge. Cap0 is further modified by 2′-*O*-methylation of the next two riboses, yielding 'cap1' (m7GpppNmN) and 'cap2' (m7GpppNmNm). However, some viral RNAs lack 2′-*O*-methylation, whereas others contain only ppp- at their 5′-end. Interferon-induced proteins with tetratricopeptide repeats (IFITs) are highly expressed effectors of innate immunity that inhibit viral replication by incompletely understood mechanisms. Here, we investigated the ability of IFIT family members to interact with cap1-, cap0- and 5′ppp- mRNAs and inhibit their translation. IFIT1 and IFIT1B showed very high affinity to cap-proximal regions of cap0-mRNAs ($K_{1/2,app}$ ~9 to 23 nM). The 2′-*O*-methylation abrogated IFIT1/mRNA interaction, whereas IFIT1B retained the ability to bind cap1-mRNA, albeit with reduced affinity ($K_{1/2,app}$ ~450 nM). The 5′-terminal regions of 5′ppp-mRNAs were recognized by IFIT5 ($K_{1/2,app}$ ~400 nM). The activity of individual IFITs in inhibiting initiation on a specific mRNA was determined by their ability to interact with its 5′-terminal region: IFIT1 and IFIT1B efficiently outcompeted eIF4F and abrogated initiation on cap0-mRNAs, whereas inhibition on cap1- and 5′ppp- mRNAs by IFIT1B and IFIT5 was weaker and required higher protein concentrations.

INTRODUCTION

The innate immune system initiates defensive responses to infecting viruses and bacteria by recognition of 'pathogen associated molecular patterns' (PAMPs) as 'non-self' signatures. Recognition is mediated by pattern-recognition receptors (PRRs) such as Toll-like receptors and RIG-I-like receptors (1). PAMPs specific to viral mRNAs include the double-stranded nature of RNA replicative intermediates, the absence of modified nucleosides (such as N^6-methyladenosine) and single-stranded adenosine/uridine (AU)-rich regions (1). The 5′-termini of some viral mRNAs also differ from those of cellular mRNAs. The mRNA cap consists of N7-methylguanosine linked to the first nucleotide via a 5′-5′ ppp bridge: in the minimal RNA cap structure, named 'cap0', methylation is restricted to the N7 position of the guanine base, but in higher eukaryotes, additional methylation occurs at the 2′-position of riboses of the next two nucleotides, yielding the 2′-*O*-methylated 'cap1' (m^7GpppNmN) and 'cap2' (m^7GpppNmNm) (Figure 1A). Although many viral mRNAs are also capped and 2′-*O*-methylated (2), the genomic and antigenomic RNAs of negative-stranded RNA viruses such as influenza virus (family *Orthomyxoviridae*) instead have a 5′-terminal ppp (3), whereas the genomic and subgenomic mRNAs of Sindbis virus (family *Togaviridae*) are capped but lack 2′-*O*-methylation (4,5). Nucleic acid recognition by PRRs activates signaling cascades that trigger the expression of Type 1 interferons (IFN) (6). IFN secretion spreads the defensive response to neighboring cells by binding to IFN receptors, which activates the JAK–STAT signaling pathway, leading to strong transcriptional induction of >300 genes (7). The IFN-induced tetratricopeptide repeat (IFIT) genes are among the

*To whom correspondence should be addressed. Tel: +1 718 270 1034; Fax: +1 718 270 2656; Email: tatyana.pestova@downstate.edu
Correspondence may also be addressed to Christopher U.T. Hellen. Tel: +1 718 270 1034; Fax: +1 718 270 2656; Email: christopher.hellen@downstate.edu

†These authors contributed equally to the paper as first authors.

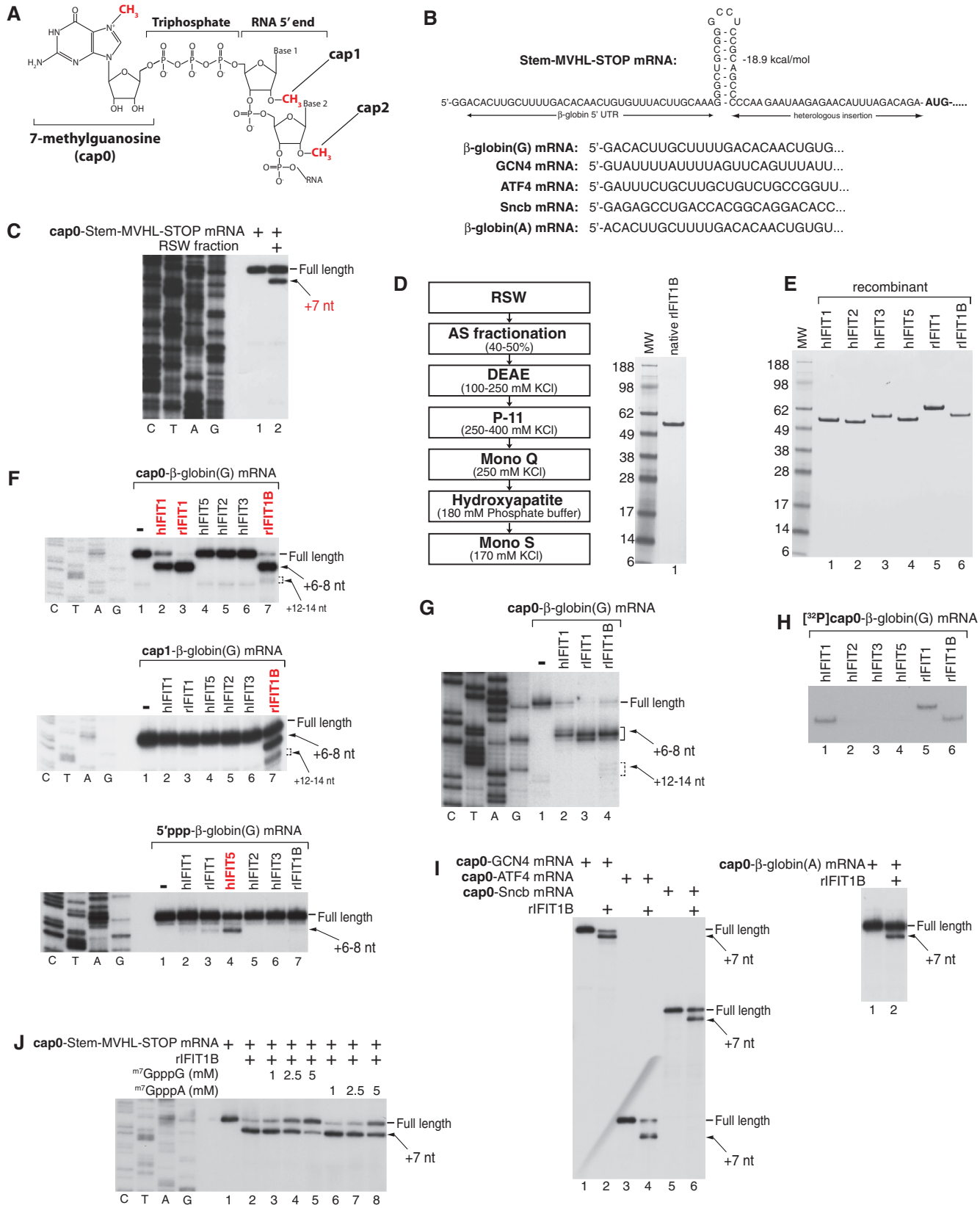

Figure 1. Specific interaction of IFIT1 and IFIT1B with the 5′-terminal regions of cap0 mRNAs. (**A**) Cap-structure. (**B**) Structure of the 5′UTR of Stem-MVHL-STOP mRNA (41) and sequences of the 5′-terminal 25 nt of β-globin(G), GCN4, ATF4, Sncb and β-globin(A) mRNAs. (**C**) Interaction of the active RRL RSW fraction with cap0-Stem-MVHL-STOP mRNA assayed by primer extension. The toe-print induced by the interaction is indicated. (**D**) Left panel: scheme for purification of IFIT1B from RRL. Right panel: purified native rIFIT1B resolved by SDS–PAGE. (**E**) Purified recombinant hIFIT1, hIFIT2, hIFIT3, hIFIT5, rIFIT1 and rIFIT1B resolved by SDS–PAGE. (**F** and **G**) Interaction of hIFIT1, hIFIT2, hIFIT3,

(continued)

most strongly induced by IFN treatment (e.g. 8,9), for example leading to the cytoplasmic accumulation of $>1 \times 10^6$ IFIT1 molecules per cell (10). Their abundance would be consistent with IFIT proteins having an executive function rather than a signaling role in innate immunity.

The IFIT family arose by gene duplication and is conserved in vertebrates (11–13). Most mammals encode IFIT1, IFIT2, IFIT3 and IFIT5, with the exception of mice and rats (which lack IFIT5) and horses (which lack IFIT1), but many species also have additional IFIT-like genes, encoding IFIT1B (in humans, mice and rabbits), IFIT1C (in mice), IFIT3B (in dogs and mice) and IFIT5-like proteins (in dogs and rabbits). IFIT proteins have molecular weights ranging between 47 and 72 kDa, and contain up to 11 tetratricopeptide repeat (TPR) motifs (14) that form a series of tandem antiparallel α-helices extending over their entire length. The regular repeating relationship between TPRs is disrupted by two insertions in IFIT2 and IFIT5, so that the TPRs form three distinct subdomains producing a V-shaped clamp-like structure (15–18). The concave surface of subdomain II, the 'pivot' helices between subdomains II and III and the N-terminal TPRs of subdomain III form a deep cylindrical cavity that is lined with positively charged residues (16–18). Whereas IFIT5 is a monomer, IFIT2 forms a domain-swapped homodimer in a manner that may account for conformational switching of subdomains during binding of ligands (15) and for homo- and heterodimerization of human IFITs 1, 1B, 2 and 3 (10,18). The functional importance of homo- and heterodimerization of IFITs is unknown.

The promoters of most IFIT genes contain one to four IFN-stimulated response elements (ISRE), typically located within 200 bp upstream of the transcription start site, that are recognized by IFN regulatory factors, leading to rapid induction of transcription. A few IFIT genes, including human IFIT1B, lack ISRE-containing promoters and are not transcriptionally induced by IFN or dsRNA (11,12). Sequence similarity between the different IFIT proteins within a species is high (44–98% identity) (11), but they are differentially expressed depending on the cell and tissue type, respond differently to IFN and different viruses, and have different effects on replication of individual viruses, suggesting that different IFITs have non-redundant functions in the host response to viral infection (e.g. 19–23).

Different IFIT members have been reported to inhibit viral replication through various mechanisms. Thus, IFIT3 and IFIT5 potentiate antiviral signaling (24,25), whereas some reports indicate that IFIT1 exhibits the opposite modulatory effect (26). IFIT2, on the other hand, has been shown to promote apoptosis via a mitochondrial pathway (27,28). However, the principal antiviral function of IFITs is thought to involve inhibition of viral translation. Over-expression of human IFIT1 in HT1080 cells reduced overall translation by ~40%, and addition of recombinant human IFIT1 and IFIT2 abrogated cap-dependent translation in rabbit reticulocyte lysate (RRL) (29). Originally, their mechanism of action was reported to involve interaction with and impairment of the functions of eukaryotic initiation factor eIF3 (30,31), a large multisubunit factor that binds to the ribosomal 40S subunit and promotes recruitment of mRNA and the eIF2•GTP/initiator tRNA (Met-$tRNA_i^{Met}$) ternary complex (32,33). However, subsequent studies were unable to confirm the repression of translation in RRL by 35 μM IFIT2 (10) or the interaction of IFIT2 with eIF3 (15).

More recent reports have focused on the interactions of IFITs with RNA, which could impair translation more directly, by sequestering tRNA or viral mRNA, or abrogate replication by binding to genomic/antigenomic RNAs. Determination of the crystal structure of IFIT2 showed that it has a positively charged RNA-binding channel on the inner surface of its carboxy-terminal subdomain that binds AU-rich RNAs (15), whereas IFIT5 has a deep positively charged RNA-binding pocket that can accommodate single-stranded nucleic acid with a 5′-terminal ppp. The crystal structures of IFIT5 bound to short 5′ppp-RNA oligoribonucleotides revealed that the 5′-terminal phosphate and four adjacent nucleotides bind to conserved residues in this cavity in a sequence-independent manner, inducing closure of the cavity (16). Non-specific binding of IFIT5 to a variety of short cellular RNAs, including initiator tRNA, has also been reported (17,34). Positively charged amino acid residues that influence binding of initiator tRNA map to a broad surface, including elements of domain II and the 'pivot' helices between it and domain III (17).

Human IFIT1 was previously reported to specifically bind 5′ppp-ssRNAs with moderate affinity ($K_d \sim 250$ nM) (10). Two independent groups have recently reported specific interaction of human IFIT1 with cap0-RNAs (35,36). These latter reports support our current finding, using a novel equilibrium-based binding assay, that human IFIT1, rabbit IFIT1 and rabbit IFIT1B specifically bind to cap-proximal regions of cap0-mRNAs with very high affinity ($K_{1/2,app} \sim 9$ to 23 nM). This enables them to compete efficiently with eIF4F and thus to inhibit translation initiation on cap0-mRNAs through sequestration. Molecular modeling and mutagenesis of human IFIT1 suggest that the ppp moiety of cap0 interacts with an extended cleft leading to a pocket that binds the N7-methylguanosine portion of the cap

Figure 1. Continued
hIFIT5, rIFIT1 and rIFIT1B (400 nM) with cap0-, cap1- and 5′ppp- β-globin(G) mRNAs assayed by primer extension. Toe-prints induced by the IFIT/mRNA interaction are indicated. For better resolution of toe-prints, primer extension in panel (G) was performed using a primer that is closer to the 5′-end of mRNA. (**H**) UV cross-linking of hIFIT1, hIFIT2, hIFIT3, hIFIT5, rIFIT1 and rIFIT1B with [^{32}P]cap-labeled cap0-β-globin(G) mRNA. (**I**) Interaction of rIFIT1B (300 nM) with cap0- GCN4, ATF4, Sncb and β-globin(A) mRNAs. Toe-prints caused by the rIFIT1B/mRNA interaction are indicated. (**J**) Competition between rIFIT1B (150 nM) and m^7GpppG or m^7GpppA dinucleotides for binding to cap0-Stem-MVHL-STOP mRNA (20 nM). The toe-print induced by the rIFIT1B/mRNA interaction is indicated.

structure. Whereas the specific and stable interaction of IFIT1 with cap0-mRNA may account for its ability to inhibit translation and thus impair replication of specific viruses, the observation that IFIT1B, which lacks an ISRE-containing promoter and is not transcriptionally induced by IFN or dsRNA, also binds cap0-mRNAs suggests that it might regulate translation of specific cellular mRNAs in circumstances that are unrelated to the innate immune response.

MATERIALS AND METHODS

Plasmids

Expression vectors for eIF1 and eIF1A (37), eIF4A and eIF4B (38), eIF4E (39), hIFIT1 (17), hIFIT2 (10), hIFIT3 (10), hIFIT5 (17) and *Escherichia coli* methionyl tRNA synthetase (40), as well as transcription vectors for Stem-MVHL-STOP mRNA (41), $tRNA_i^{Met}$ (42), $tRNA^{Leu}$ and $tRNA^{His}$ (43) have been described. A transcription vector for $tRNA^{Lys}$ was made by inserting its DNA sequence flanked by a T7 promoter and a FokI restriction site into pUC57 (GenScript). The transcription vectors for β-globin, ATF4, GCN4 and Sncb mRNAs were made by inserting DNA sequences (corresponding to their 5′-terminal 235, 442, 600 and 247 nt, respectively) flanked by a T7 promoter and HindIII, EcoRV, EcoRV and HindIII restriction sites, respectively, into pUC57 (GenScript). pET-28a(rIFIT1) for expression of rIFIT1 (NCBI Reference sequence XP_002718421.1) and pET16b(rIFT1B) for expression of rIFIT1B (NCBI Reference sequence XP_002718420.1) were made by Biomatik Inc. (Cambridge, ON, Canada) by inserting synthetic DNA sequences between Nhe1 and BamH1 sites of pET28a(+) and Nde1 and BamH1 sites of pET16b (Novagen), respectively. pET16b(hIFIT1B) for expression of hIFIT1B was made by inserting a DNA fragment amplified by polymerase chain reaction from plasmid HsCD00342660/MGC: 168989 (Genbank Acc. No. BC137368) from the DF/HCC DNA Resource Core (Harvard Medical School) between Nde1 and BamH1 sites of pET16b. hIFIT1 mutants were generated by NorClone Biotech Laboratories (London, ON, Canada) using a *wt* IFIT1 expression vector (17). mRNAs and tRNAs were *in vitro* transcribed using T7 polymerase. For EMSA, $tRNA_i^{Met}$ and RNA comprising 62 5′-terminal nucleotides of cap0-β-globin(G) mRNA were transcribed in the presence of [α^{32}P]ATP, [α^{32}P]GTP and [α^{32}P]CTP (6000 Ci/mmol).

Purification of initiation factors, 40S ribosomal subunits and aminoacylation of $tRNA_i^{Met}$

Native 40S ribosomal subunits, eIF2, eIF3 and eIF4F, and recombinant eIF1, eIF1A, eIF4A, eIF4B, eIF4E and *E. coli* methionyl tRNA synthetase were purified as described in (40,44,45). *In vitro* transcribed $tRNA_i^{Met}$ was aminoacylated using *E. coli* methionyl tRNA synthetase (45). For experiments on 43S complex formation, aminoacylation was done in the presence of [^{35}S]Met.

Purification of native rIFIT1B

Native rIFIT1B was purified from RRL on the basis of its activity in binding to cap0-Stem-MVHL-STOP mRNA, which was monitored by primer extension. The 40–50% ammonium sulfate precipitation fraction of the 0.5 M KCl ribosomal salt wash that was prepared from 1 l of RRL (Green Hectares, Oregon, WI, USA) (43) was dialyzed against buffer A (20 mM Tris–HCl, pH 7.5, 10% glycerol, 2 mM DTT, 0.1 mM EDTA) + 100 mM KCl and applied to a DE52 column equilibrated with buffer A + 100 mM KCl. rIFIT1B was eluted by buffer A + 250 mM KCl. This fraction was applied to a P11 column equilibrated with buffer A + 100 mM KCl, and rIFIT1B was eluted between 250 and 400 mM KCl. This fraction was applied to a FPLC MonoQ HR 5/5 column. Fractions were collected across a 100–500 mM KCl gradient. rIFIT1B was eluted at ~250 mM KCl. rIFIT1B-containing fractions were applied to a hydroxyapatite column. Fractions were collected across a 20–500 mM phosphate buffer gradient. rIFIT1B was eluted at ~180 mM phosphate buffer. rIFIT1B-containing fractions were applied to a FPLC MonoS HR 5/5 column. Fractions were collected across a 50–500 mM KCl gradient. rIFIT1B was eluted at ~170 mM KCl. rIFIT1B-containing fractions were concentrated on Microcon YM30 (Millipore).

Purification of recombinant IFITs

Recombinant wild-type hIFIT1, hIFIT2, hIFIT3, hIFIT5, rIFIT1 and rIFIT1B, and hIFIT1 mutants were expressed in 1 l of BL21 DE3 Star *Escherichia coli* (Invitrogen). Cells were grown at 37°C to an OD_{600} of 0.6. Protein production was induced by the addition of 0.2 mM IPTG, after which incubation continued for 16 h at 16°C. Proteins were isolated by affinity chromatography on Ni-NTA-agarose followed by FPLC on a MonoQ HR5/5 column. After that, rIFIT1B was additionally purified by FPLC on a Superdex 200 column.

Capping of mRNA

mRNA (30 μg) was included in a capping reaction performed using the T7 mScript Standard mRNA Production System (Cellscript, Madison, WI, USA). Cap0- or cap1- mRNAs were generated by omission or inclusion of 2′-*O*-methyltransferase in the capping reaction, respectively. N7-unmethylated cap0-mRNA was generated by performing the capping reaction in the absence of S-adenosyl-methionine. For UV cross-linking experiments, capping was performed in the presence of [α^{32}P]GTP.

Analysis of the IFIT/mRNA interaction by primer extension inhibition

Cap0-, cap1- and 5′ppp- β-globin(G) mRNAs (0.5 nM) were incubated with IFIT proteins (at concentrations indicated in Figures and Figure Legends) for 10 min at 37°C in 100 μl reaction mixtures containing buffer B (20 mM Tris, pH 7.5, 100 mM KCl, 2.5 mM $MgCl_2$, 1 mM ATP, 0.2 mM GTP, 1 mM DTT and 0.25 mM

spermidine). In competition experiments, reaction mixtures were also supplemented with m^7GpppG, m^7GpppA, eIF4E, eIF4F or tRNAs at concentrations indicated in Figures and Figure Legends. mRNA/IFIT association was analyzed by primer extension inhibition, using avian myeloblastosis virus reverse transcriptase (AMV-RT) (2.5 U) and ^{32}P-labeled primer in the presence of 4 mM $MgCl_2$ and 0.5 mM dNTPs. cDNA products were resolved in a 6% acrylamide sequencing gel and visualized by autoradiography. The intensities of full-length and IFIT induced stops were quantified using an Amersham Storm 860 Phosphoimager.

Electrophoretic mobility shift assay

Electrophoretic mobility shift assay (EMSA) was performed essentially as described (46). IFIT proteins (at concentrations indicated in Figures and Figure Legends) were incubated with ^{32}P-labeled $tRNA_i^{Met}$ or cap0-RNA comprising 62 5′-terminal nucleotides of cap0-β-globin(G) mRNA (0.5 nM) at 37°C for 10 min in 10 µl reaction mixtures containing buffer B. After addition of 2 µl of loading buffer (60% glycerol, 0.01% Bromophenol Blue), samples were applied to non-denaturing 6% acrylamide gels and subjected to electrophoresis using 90 mM Tris, 90 mM boric acid and 1 mM EDTA running buffer. Bound and unbound fractions were visualized by autoradiography.

UV cross-linking

[^{32}P]cap-labeled cap0-β-globin(G) mRNA (50 nM) was incubated with IFIT proteins (200 nM) for 10 min at 37°C in 20 µl reaction mixtures containing buffer B and subjected to irradiation on ice for 20 min at 254 nm using a UV Stratalinker (Stratagene). Samples were treated with RNAses A, V1 and T1 before separation on NuPAGE 4-12% Bis-Tris Gel (Invitrogen). Cross-linked proteins were visualized by autoradiography.

Analysis of 48S initiation complex formation

48S complexes were assembled by incubation of cap0-β-globin(G), cap1-β-globin(G) or 5′ppp-β-globin(G) mRNAs (12.5 nM) with 40 S subunits (110 nM), eIF2 (250 nM), eIF3 (150 nM), eIF1 (300 nM), eIF1A (300 nM), eIF4A (400 nM), eIF4B (150 nM), eIF4F (150 nM) and Met-$tRNA_i^{Met}$ (200 nM) in the presence or in the absence of IFITs (at concentrations indicated in Figures and Figure Legends) for 10 min at 37°C in 20 µl reaction mixtures containing buffer B. 48S complex formation was analyzed by toe-printing (43) using AMV-RT (2.5 U) and ^{32}P-labeled primer at 12 mM $MgCl_2$ to stabilize 48S complexes. cDNA products were resolved in a 6% acrylamide sequencing gel and visualized by autoradiography. The intensities of full length and IFIT induced stops were quantified using an Amersham Storm 860 Phosphoimager.

Ribosomal association of IFITs

IFIT proteins (300 nM) were incubated with 40S ribosomal subunits (160 nM) for 15 minutes at 37°C in 200 µl reaction mixtures containing buffer B. The reaction mixtures were then subjected to centrifugation through 10–30% sucrose density gradients in a Beckman SW55 rotor at 53 000 rpm for 90 min. Fractions that corresponded to ribosomal complexes were trichloroacetic acid precipitated and analyzed by sodium dodecyl sulphate–polyacrylamide gel electrophoresis SDS–PAGE using the NuPAGE 4–12% Bis-Tris Gel System (Invitrogen) with subsequent fluorescent SYPRO (Invitrogen) staining.

Analysis of 43S preinitiation complex formation

43S complexes were assembled from 40S ribosomal subunits (80 nM), eIF2 (120 nM), eIF3 (200 nM), eIF1 (500 nM), eIF1A (500 nM) and [^{35}S]Met-$tRNA_i^{Met}$ (100 nM; 350 000 cpm) in the presence or in the absence of hIFIT1 or rIFIT1B (300 nM) in 200 µl reaction mixtures containing buffer B. Before addition of other components, IFITs were preincubated with either 40S subunits, [^{35}S]Met-$tRNA_i^{Met}$, or [^{35}S]Met-$tRNA_i^{Met}$ and eIF2 for 10 min at 37°C. After assembly of final mixtures, incubation continued for an additional 10 min. Assembled complexes were separated by centrifugation through 10–30% SDGs as described above. 43S complex formation was analyzed by scintillation counting of an aliquot of each fraction.

Native gel electrophoresis

The oligomerization status of different IFIT proteins was analyzed using the NativePAGE Gel system (Invitrogen) as per the manufacturer's instructions. A total of 500 ng of recombinant hIFIT1, hIFIT2, hIFIT3, hIFIT 5, rIFIT1 and rIFIT1B were separated on a 4–16% non-denaturing Bis-Tris gradient gel (Invitrogen). The gel was run in 50 mM Bis-Tris and 50 mM Tricine at pH 8. Coomassie G-250 (0.02%) (Invitrogen) was included as a charge shift molecule in the cathode buffer. After electrophoresis, protein bands were visualized using the Novex colloidal blue staining kit (Invitrogen).

RESULTS

IFIT1 and IFIT1B, but not IFIT2, IFIT3 and IFIT5, interact specifically with the 5′-terminal regions of cap0 mRNAs

Routine activity testing during purification of the eukaryotic ribosome recycling factor ABCE1 (47) from RRL, which involved toe-printing of ribosomal complexes formed on cap0-Stem-MVHL-STOP mRNA (a derivative of β-globin mRNA, containing two 5′-terminal guanine nucleotides and a stable stem in the middle of the 5′UTR; Figure 1B; 41), revealed that some fractions induced strong arrest of reverse transcriptase (RT) seven nucleotides downstream of the 5′-end of the mRNA (Figure 1C), indicating a stable and specific interaction between constituents of these fractions and the 5′-terminal region of cap0 mRNA. Extensive purification of the active component (Figure 1D, left panel) yielded an apparently homogenous ~55 kDa protein (Figure 1D, right panel), which was identified as IFIT1B

(Supplementary Table S1). To determine whether this mRNA-binding activity was specific for rabbit IFIT1B, the following members of the IFIT family were expressed and purified in recombinant form: human (h) IFIT1, IFIT2, IFIT3 and IFIT5, and rabbit (r) IFIT1 and IFIT1B (Figure 1E). Attempts to express recombinant hIFIT1B did not yield a soluble protein. To investigate the influence of the nature of mRNA nucleotides on IFIT/mRNA binding, five mRNAs with different 5′-terminal sequences were employed: β-globin(G) and β-globin(A) mRNAs with a 5′-terminal guanosine or adenosine, respectively, GCN4 mRNA, ATF4 mRNA and Sncb (beta-synuclein) mRNA (Figure 1B).

At 400 nM, hIFIT1, rIFIT1 and rIFIT1B (but not hIFIT2, hIFIT3 or hIFIT5) induced +7 nt toe-prints on cap0-β-globin(G) mRNA (Figure 1F, top panel). Although the +7 nt stop was the most prominent in all cases, the intensity of additional stops at flanking +6 and +8 positions differed: the strongest stop at +8 nt was induced by rIFIT1, whereas the +6 nt stop was most obvious in the case of hIFIT1 (Figure 1G). This subtle difference suggests that the strength of the mRNA/IFIT interaction at the 3′-border of the interacting mRNA region varies between the three IFITs. In the case of rIFIT1B, additional low-intensity toe-prints were also observed at +12−14 positions. Binding of hIFIT1 and rIFIT1 was specific for cap0-β-globin(G) mRNA: no RT arrest was observed on cap1-β-globin(G) mRNA in their presence (Figure 1F, middle panel). rIFIT1B, on the other hand, was able to induce a +7 nt toe-print on cap1-β-globin(G) mRNA, but with only half the efficiency of that observed on cap0-β-globin(G) mRNA (Figure 1F, compare middle and top panels). On β-globin(G) mRNA containing a 5′-terminal ppp, a prominent toe-print at the +7 position was observed in the presence of hIFIT5, whereas hIFIT1, rIFIT1 and rIFIT1B induced only trace-level stops at this position (Figure 1F, bottom panel). Interestingly, toe-prints induced by hIFIT1 on cap0-β-globin(G) mRNA, and to a greater extent toe-prints induced by rIFIT1B and hIFIT5 on cap1- and on 5′ppp- β-globin(G) mRNAs, respectively, were sensitive to elevation of [Mg^{2+}] above 6 mM during the primer extension stage, which most likely indicates that at these [Mg^{2+}], RT displaces these IFITs from mRNA (PK, TRS and TVP, unpublished data). No specific toe-prints were observed in the presence of hIFIT2 and hIFIT3, irrespective of the structure present at the 5′-end of mRNA (Figure 1F, all panels). Consistently, hIFIT1, rIFIT1 and rIFIT1B, but not hIFIT2, hIFIT3 and hIFIT5 cross-linked to [^{32}P]cap-labeled cap0-β-globin(G) mRNA (Figure 1H). Despite sequence differences in the 5′-terminal region of the various tested cap0 mRNAs (Figure 1B), hIFIT1, rIFIT1 and rIFIT1B specifically interacted with them all (shown for rIFIT1B in Figure 1I). Interestingly, the m^7GpppG and m^7GpppA dinucleotides were only weak competitors of IFIT/cap0-mRNA binding (with m^7GpppG being slightly stronger than m^7GpppA) (shown for rIFIT1B in Figure 1J), suggesting that the IFIT/cap0-mRNA interaction extends over several cap-proximal nucleotides.

The affinities of hIFIT1, rIFIT1 and rIFIT1B for cap0 mRNAs

To determine the affinity of hIFIT1, rIFIT1 and rIFIT1B for cap0-β-globin(G) mRNA, of rIFIT1B for cap1-β-globin(G) mRNA, and of hIFIT5 for 5′ppp-β-globin(G) mRNA, the primer extension technique was employed (Figure 2A–E). Importantly, primer extension is performed under conditions of binding equilibrium, which represents a significant advantage of this method over non-equilibrium techniques such as the EMSA. Moreover, in the primer extension assay, unbound and IFIT-associated mRNAs yield sharp, distinct signals that could be quantified with high confidence. In all cases, sigmoidal binding curves were obtained. All tested IFITs bound to cap0-β-globin(G) mRNA very tightly (Figure 2A–C), with similar affinities: $K_{1/2,app} = 23 \pm 4$ nM for hIFIT1, $K_{1/2,app} = 20 \pm 1$ nM for rIFIT1 and $K_{1/2,app} = 9 \pm 2$ nM for rIFIT1B. The values of Hill coefficients $n > 1$ ($n = 1.6 \pm 0.1$ for hIFIT1, $n = 1.7 \pm 0.2$ for rIFIT1, and $n = 1.8 \pm 0.2$ for rIFIT1B) suggested some positive cooperativity in each instance. The affinities of rIFIT1B for cap1-β-globin(G) mRNA (Figure 2D; $K_{1/2,app} = 457 \pm 24$ nM) and of hIFIT5 for 5′ppp-β-globin(G) mRNA (Figure 2E; $K_{1/2,app} = 372 \pm 21$ nM) were similar, but were more than one order of magnitude lower than those of hIFIT1, rIFIT1 and rIFIT1B for cap0-β-globin(G) mRNA. No measurable stable binding to 5′ppp-β-globin(G) mRNA was observed for hIFIT1 and rIFIT1 at concentrations of up to ∼1.4 μM (Supplementary Figure S1).

Since primer extension only detects specific binding of IFITs to the cap-proximal region of mRNA and as it is highly unlikely that one IFIT molecule contains more than one such binding site, low-level positive cooperativity could potentially result only from oligomerization of IFITs at higher concentrations, if it increases the affinity of IFITs to cap0-mRNA. In native gel electrophoresis (Supplementary Figure S2), the highest degree of oligomerization was observed for rIFIT1B. hIFIT2 migrated as a dimer consistent with a previous report (15). hIFIT3 also showed a high tendency to dimerization, whereas dimerization of hIFIT1 was lower, and hIFIT5 and rIFIT1 were mostly monomeric.

Consistent with primer extension experiments (Figure 1F), EMSA also detected binding of cap0-RNA (comprising 62 5′-terminal nucleotides of cap0-β-globin(G) mRNA; Figure 2F, upper panel) only to hIFIT1, rIFIT1 and rIFIT1B (Figure 2F, four left panels), confirming that the lack of binding of hIFIT2, hIFIT3 and hIFIT5 to cap0 mRNA in primer extension experiments was not caused by displacement of IFITs by RT. The mobility of different IFIT/cap0-RNA complexes was consistent with the tendency of the particular IFIT to oligomerize (Supplementary Figure S2). Thus, increasing hIFIT1 concentrations resulted in the progressive appearance of a slower migrating complex, likely corresponding to hIFIT1 dimers (Figure 2F, first panel from the left), whereas no dimers were observed in the case of rIFIT1 (Figure 2F, second panel from the left). rIFIT1B, on the other hand, did not form monomeric complexes, and even

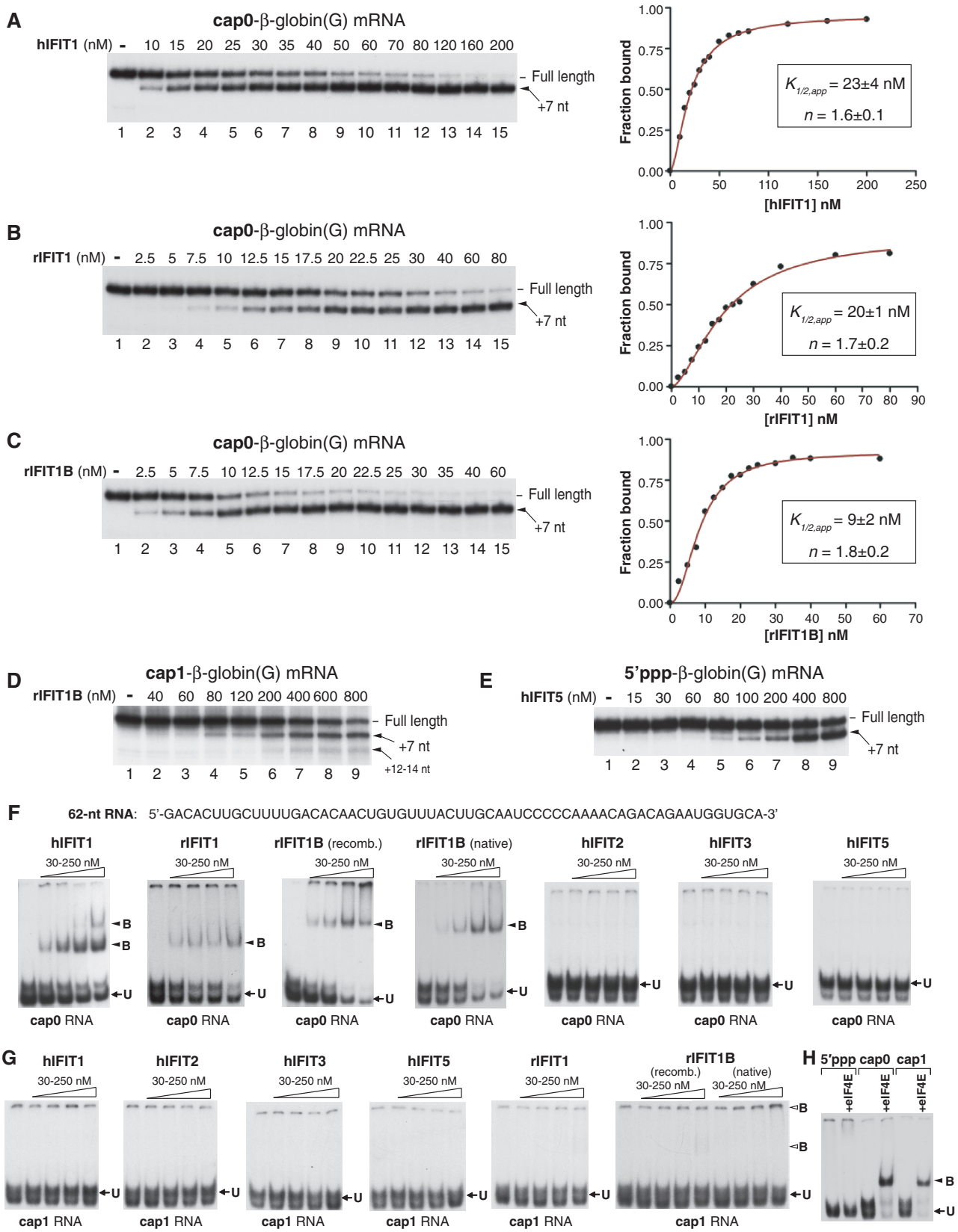

Figure 2. Binding constants for hIFIT1, rIFIT1 and rIFIT1B association with cap0 mRNAs. (**A–C**) Left panels: representative gels of titration of the association of hIFIT1, rIFIT1 and rIFIT1B with cap0-β-globin(G) mRNA assayed by primer extension. Toe-prints induced by the IFIT/mRNA interaction are indicated. Right panels: corresponding plots of the dependence of the fraction of IFIT-bound mRNA on the concentration of IFITs. The curves were fitted to the non-linear Hill equation ($Frac^{[bound]} = [IFIT]^n \bullet Frac^{[bound]}_{max} / ([IFIT]^n + K^n_{1/2,app})$) using GraphPad Prism software. Dissociation constant ($K_{1/2,app}$) and Hill coefficient (n) calculated on the basis of at least three independent experiments are shown in the inset boxes.

(continued)

at the lowest concentrations migrated as a dimer, with the recombinant form having a stronger tendency to oligomerize at higher concentrations and to form high molecular weight complexes that migrated close to the start (Figure 2F, third and fourth panels from the left). Again, as in primer extension experiments (Figure 1F), no binding to cap1-RNA was observed for hIFIT1, rIFIT1, hIFIT2, hIFIT3 and hIFIT5, and only a small amount of complexes formed in the case of rIFITB at the highest concentration of the protein (Figure 2G). In control experiments, eIF4E bound to both cap0- and cap1- RNAs (Figure 2H).

Sensitivity of hIFIT1, rIFIT1 and rIFIT1B to N7-methylation of the cap, and their competition with eIF4E and eIF4F for binding to cap0-mRNAs

Next, we investigated the requirement for N7-methylation of the cap for binding of hIFIT1, rIFIT1 and rIFIT1B to cap0-β-globin(G) mRNA. Although N7-methylation was not essential for binding by any of the IFITs (Figure 3A–C), differences between them were nevertheless observed. Thus, at lower concentrations, binding of hIFIT1 to unmethylated cap0-globin(G) mRNA appeared to be more efficient, but in contrast to binding to methylated mRNA, did not reach saturation at higher concentrations (Figure 3A), likely due to a greater degree of displacement of IFIT by RT, which prevented accurate determination of the binding constant. In contrast, binding of rIFIT1 to unmethylated cap0-globin(G) mRNA was weaker ($K_{1/2,app} = 81 \pm 5$ nM) than to the methylated equivalent (Figure 3B). The highest dependence on N7-methylation was observed for rIFIT1B, which bound to unmethylated cap0-globin(G) mRNA with the lowest $K_{1/2,app}$ of 340 ± 15 nM (Figure 3C).

In competition experiments, association of hIFIT1 and rIFIT1B with N7-methylated cap0-β-globin(G) mRNA was not affected by 5- or even 10-fold excess of eIF4E (Figure 3D) or eIF4F (Figure 3E), irrespective of the presence of ATP or ADPNP in the reaction mixture.

The effect of hIFIT1, hIFIT2, hIFIT3, hIFIT5, rIFIT1 and rIFIT1B on 48S initiation complex formation on cap0-, cap1- and 5′ppp- mRNAs

The influence of IFITs on translation initiation was investigated using an *in vitro* reconstituted translation system. 48S complexes were assembled from individual purified 40S subunits, Met-tRNA$_i^{Met}$, eIF2, eIF3, eIF1, eIF1A, eIF4A, eIF4B and eIF4F on cap0-, cap1- and 5′ppp- β-globin(G) mRNAs in the presence and absence of IFITs, and analyzed by toe-printing. Although IFIT/mRNA complexes (particularly rIFIT1B/cap1-mRNA and hIFIT5/5′ppp-mRNA complexes) were sensitive to dissociation by RT at high Mg^{2+} concentrations, the toe-printing stage in these experiments was nevertheless performed at an elevated Mg^{2+} concentration in order to 'freeze' 48S complexes after their assembly. As a result, toe-prints corresponding to rIFIT1B/cap1-mRNA and hIFIT5/5′ppp-mRNA binary complexes were not apparent in these experiments. At 800 nM, hIFIT1, rIFIT1 and rIFIT1B nearly abrogated 48S complex formation on cap0-β-globin(G) mRNA, whereas hIFIT2, hIFIT3 and hIFIT5 did not influence the level of 48S complex formation (Figure 4A). In addition, consistent with their binding to cap1- and 5′ppp- mRNAs (Figures 1F, 2D and E), rIFIT1B and hIFIT5 strongly inhibited 48S complex formation on cap1-β-globin(G) and 5′ppp-β-globin(G) mRNAs, respectively (Figure 4B and C). Thus, the ability of different IFITs to inhibit 48S complex formation on a specific mRNA correlated with their ability to interact with its 5′-terminal region (Figures 1F and 2A–E). Titration experiments showed that 48S complex formation on cap0-β-globin(G) mRNA was sensitive even to low concentrations of hIFIT1, rIFIT1 and rIFIT1B (Figure 4D and E), whereas inhibition of 48S complex formation on cap1-β-globin(G) and 5′ppp-β-globin(G) mRNAs by rIFIT1B and hIFIT5 required higher protein concentrations (Figure 4F and G) (quantitative comparison shown in Figure 4H). Notably, the IC_{50} for IFIT1B on cap1-β-globin(G) was ~2-fold lower than would be anticipated on the basis of the $K_{1/2,app}$, which suggests that in this particular case, primer extension might have yielded an underestimated $K_{1/2,app}$ value due to protein displacement by RT.

Identification of critical residues required for interaction of hIFIT1 with cap0-mRNAs

The crystal structure of hIFIT5 (Figure 5A) in complex with short RNAs carrying 5′ppp moieties revealed a narrow, highly charged ssRNA binding cleft (16). A number of positively charged residues interact with the phosphate backbone of RNA and are critical for ssRNA binding by the protein (Figure 5A, right top panel). The 5′ppp is recognized by a network of interactions at the rear of the binding cleft such that there is insufficient space to accommodate the N7-methylguanosine portion of the cap structure. However, our structural evaluation indicated that N7-methylguanosine could be accommodated in the cleft with minimal disruption to RNA phosphate backbone and base binding if the trajectory of the ppp in the hIFIT1 binding pocket differed from that in hIFIT5 (Figure 5A, right bottom panel). To investigate whether the 5′-terminal region of cap0-mRNA occupies the same cleft in hIFIT1 as the 5′-terminal region of 5′ppp-RNA in hIFIT5, we generated a panel of 12 hIFIT1 mutants (Figure 5B; Supplementary Figure S3)

Figure 2. Continued
(**D** and **E**) Representative gels of titration of the association of (D) rIFIT1B and (E) hIFIT5 with cap1- and 5′ppp- β-globin(G) mRNAs, respectively, assayed by primer extension. Toe-prints induced by the IFIT/mRNA interaction are indicated. (**F** and **G**) Binding of hIFIT1, hIFIT2, hIFIT3, hIFIT5, rIFIT1 and rIFIT1B (30, 60, 120, 250 nM) to ^{32}P-labeled cap0- (F) and cap1- (G) RNAs comprising 5′-terminal 62 nt of β-globin(G) mRNA (F, upper panel) assayed by EMSA. (**H**) Binding of eIF4E (2 μM) to ^{32}P-labeled cap0-, cap1- and 5′ppp- 62 nt-long RNA (F, upper panel) assayed by EMSA. 'U' and 'B' indicate unbound and bound RNAs, respectively (F–H).

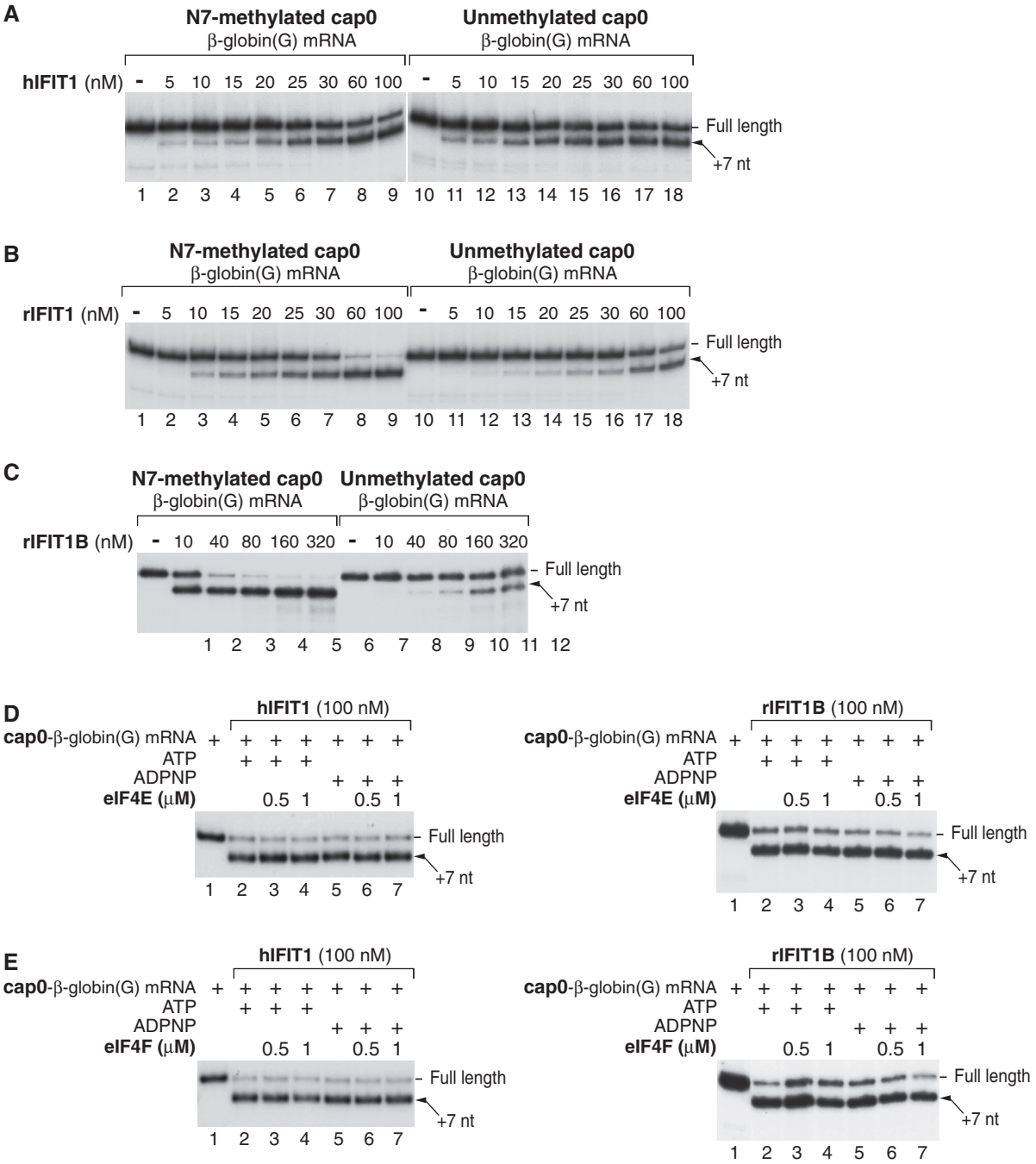

Figure 3. The influence of N7-methylation on the association of hIFIT1, rIFIT1 and rIFIT1B with cap0 mRNA. (**A–C**) Binding of (A) hIFIT1, (B) rIFIT1 and (C) rIFIT1B to N7-methylated and unmethylated cap0-β-globin(G) mRNAs, assayed by primer extension. (**D** and **E**) Competition of hIFIT1 (left panels) and rIFIT1B (right panels) with eIF4E (D) and eIF4F (E) for binding to cap0-β-globin(G) mRNA, assayed by primer extension. Toe-prints induced by the IFIT/mRNA interaction are indicated (A–E).

and examined their ability to bind cap0-β-globin(G) mRNA and inhibit 48S complex formation on it.

One set of mutations consisted of substitutions of residues (D34, K259 and R262), whose equivalents interact with 5′ppp-RNA in the hIFIT5 crystal structure and have been found to influence binding of RNA to hIFIT5 or hIFIT1. E33 of hIFIT5 interacts with an ion, likely Mg^{2+}, that bridges the α- and γ-phosphates of 5′ppp-RNA (16), and substitution by Ala of the equivalent D34 in hIFIT1 abrogated its ability to bind to cap0-β-globin(G) mRNA (as evidenced by the disappearance of the toe-print at the +6−7 positions; Figure 5C) and to inhibit 48S complex formation (Figure 5D). This D34A substitution in hIFIT1 and to a lesser extent the analogous E33 substitution in hIFIT5 inhibited their binding to 5′ppp-RNA (16). In hIFIT5, K257 and R260 make a salt bridge with the 5′-phosphate of the third nucleotide and are required for binding to 5′ppp-RNA (16,18).

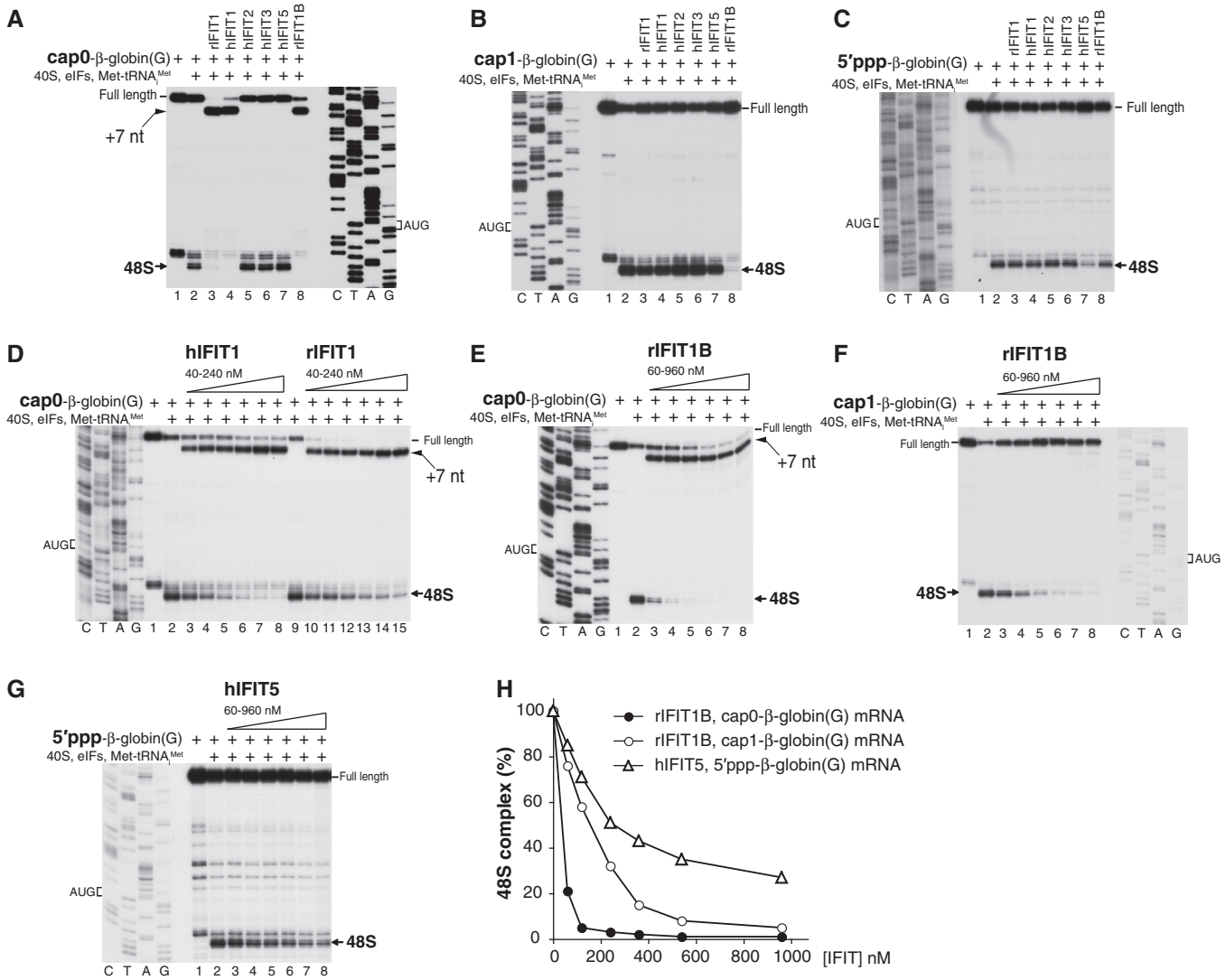

Figure 4. Inhibition of 48S complex formation on cap0-, cap1- and 5′ppp- mRNAs by hIFIT1, hIFIT2, hIFIT3, hIFIT5, rIFIT1 and rIFIT1B. (**A–C**) Toe-printing analysis of 48S complex formation on (A) cap0-, (B) cap1- and (C) 5′ppp- β-globin(G) mRNAs from 40S subunits, eIFs 2, 3, 1, 1A, 4A, 4B and 4F, and Met-tRNA$_i^{Met}$ in the presence or absence of 800 nM hIFIT1, hIFIT2, hIFIT3, hIFIT5, rIFIT1 or rIFIT1B. The positions of AUG codons and toe-prints corresponding to 48S complexes or mRNA/IFIT contacts are indicated. (**D–G**) Titration of inhibition of 48S complex formation on (D and E) cap0-, (F) cap1- and (G) 5′ppp- β-globin(G) mRNAs by hIFIT1 (40, 60, 80, 120, 160 and 240 nM), rIFIT1 (40, 60, 80, 120, 160 and 240 nM), rIFIT1B (60, 120, 240, 360, 540 and 960 nM) or IFIT5 (60, 120, 240, 360, 540 and 960 nM), assayed by toe-printing. Positions of AUG codons, and toe-prints corresponding to 48S complexes and IFIT/mRNA contacts are indicated. (**H**) Comparison of inhibition of 48S complex formation by rIFIT1B on cap0- and cap1- β-globin(G) mRNAs and by hIFIT5 on 5′ppp-β-globin(G) mRNA. The efficiency of 48 S complex formation in the presence of IFITs (panels E–G) was quantified relative to that in their absence, which was defined as 100%.

Similarly, K259E and R262E substitutions of equivalent residues in hIFIT1 abrogated its ability to bind to cap0-β-globin(G) mRNA and to inhibit 48S complex formation (Figure 5C and D). The neighboring R263E mutation also impaired the activity of hIFIT1 (Figure 5C and D). Thus, the residues that are involved in the interaction of IFIT5 with 5′ppp-RNA are also critical for binding of cap0 mRNA by IFIT1.

The second set of mutations targeted residues (F45, Y50, W147 and Y218), which could participate in formation of a hypothetical pocket for accommodation of N7-methylguanosine (Figure 5A, right bottom panel). W147L and Y218A substitutions completely abrogated the ability of hIFIT1 to bind to cap0-β-globin(G) mRNA and to inhibit 48S complex formation (Figure 5C and D). Interestingly, hIFIT1 mutants containing F45A or Y50A substitutions at the top of the RNA binding cleft produced only weak toe-prints at the +6−7 position (Figure 5C), but strongly inhibited 48S complex formation (Figure 5D), suggesting that they can bind cap0 RNA almost as efficiently as the *wt* protein but are more readily displaced by RT during toe-printing. The double mutation F45A/Y50A nearly abrogated the ability of hIFIT1 to bind to cap0-β-globin(G) mRNA and to inhibit 48S complex formation (Figure 5C and D). Although it cannot be strictly excluded that substitution of these hydrophobic residues could influence the structure of the pocket or even the protein, we note that these

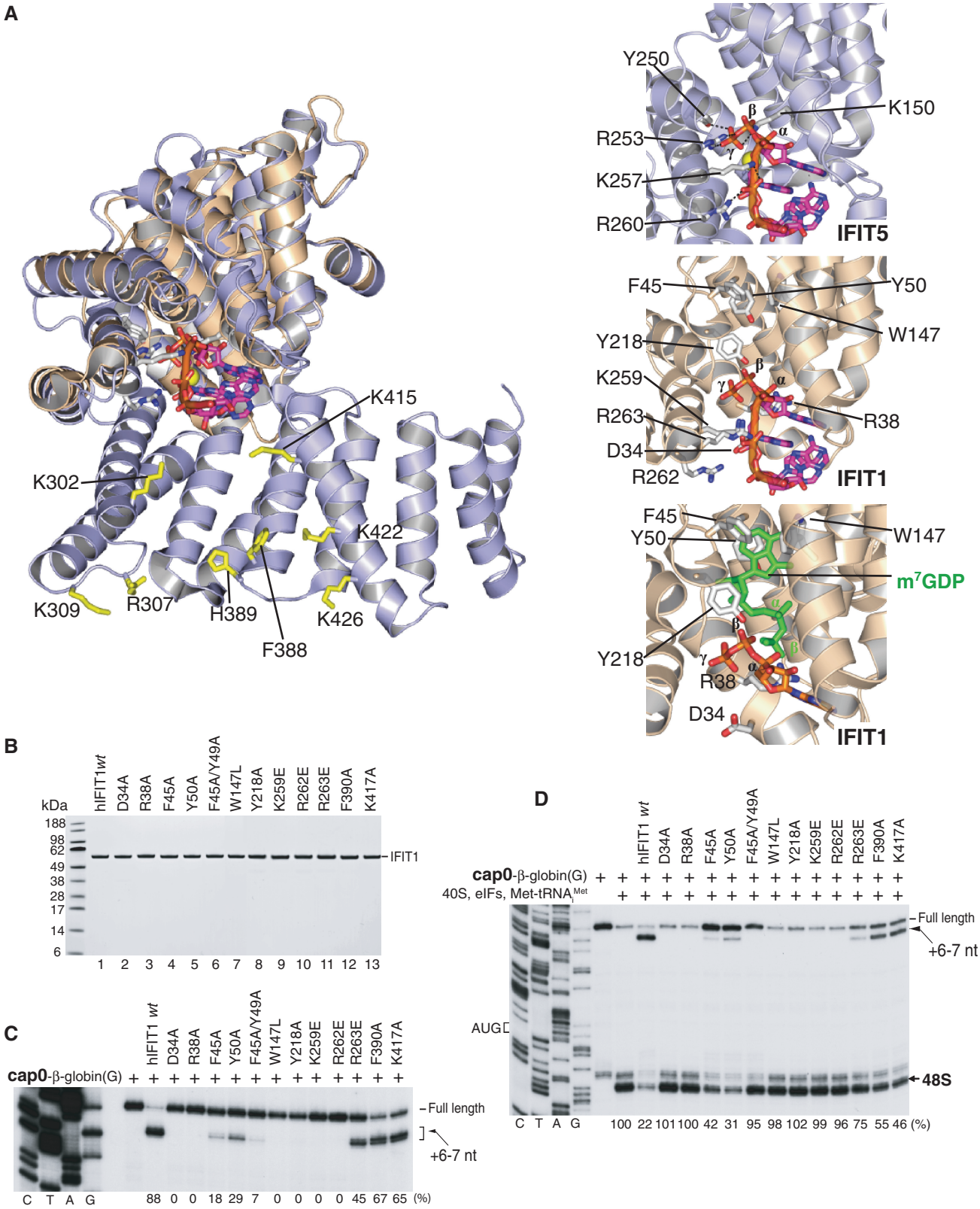

Figure 5. Activities of hIFIT1 mutants. (**A**) The location of mutated residues mapped onto the crystal structures of hIFIT5 (blue, PDB ID: 4HOT) and the N-terminal domain of hIFIT1 (light brown, PDB ID: 4HOU). Left panel: the N-terminal domain of hIFIT1 was aligned to the structure of hIFIT5. 5′ppp-AAAA RNA is shown in the nucleotide binding cleft of hIFIT5 as magenta sticks. The location of a metal ion, possibly Mg^{2+}, in the RNA binding cleft is shown as a yellow sphere. hIFIT5 residues implicated in tRNA binding by Katibah *et al.* (17), are shown as yellow sticks. Top right panel: hIFIT5 5′ppp-RNA binding cleft. The co-crystallized 5′ppp-AAAA is shown as magenta sticks. Residues that interact with the phosphate backbone and 5′-triphosphate are shown as white sticks. Middle right: 5′ppp-AAAA from the hIFIT5 co-crystal structure is modeled into the hIFIT1 RNA binding cleft. Residues mutated in hIFIT1 in this study are shown as white sticks. Bottom right: m^7GDP (green) was placed in the

(continued)

mutants all efficiently expressed and purified as soluble proteins, and behaved identically to the *wt* IFIT1 during native gel electrophoresis (Supplementary Figure S4). Taken together, the results of mutational analysis confirmed that the same RNA binding cleft in hIFIT1 is responsible for binding both 5′ppp- and cap0- RNAs, and revealed that both hydrophobic and charge–charge interactions within the cleft contribute to optimal cap0-RNA binding.

The conserved nature of the RNA-binding pockets of IFIT5 and IFIT1 raises the question of why only IFIT1 is able to interact with cap0-RNA. One obvious exception to the conserved character of the RNA binding cleft is the presence of R38 in hIFIT1 as compared to T37 at an analogous location in hIFIT5 (Figure 5A, right middle panel). In the IFIT5/RNA complex, T37 stabilizes K150, which interacts with the 5′ppp at both the β and γ positions: both residues are essential for binding of IFIT5 to 5′ppp-RNA (16). An R38A substitution abrogated the ability of hIFIT1 to bind to cap0-β-globin(G) mRNA and inhibit 48S complex formation (Figure 5C and D). The position of R38 might enable it to support an interaction between hIFIT1 and cap0 in which the location of the ppp moiety is distinct from that in the hIFIT5/5′ppp-RNA co-crystal structure. Moreover, the absence in IFIT1 of the stabilizing influence of a Thr residue at this location may free K151 (homologous to K150 in hIFIT5) to contribute to interaction with the ppp in the new trajectory.

Finally, substitution of F390 and K417, which are distal to the RNA binding cleft and located in a region that has been implicated in IFIT5's interaction with tRNA (17; Figure 5A), had a very weak effect on hIFIT1 activity (Figure 5C and D) indicating that the charged cleft is the principal determinant of binding of cap0-RNA. Interestingly, both mutations (but particularly K417A) increased the relative prominence of the +6 nt toe-print, indicating that these residues could be involved in IFIT1's interaction with nucleotides that are more distal from the 5′-end. In fact, if the positions of the first four nucleotides of cap0-RNA bound to IFIT1 are similar to those on IFIT5, then the sixth nucleotide would reach K417.

Interaction of hIFIT1, hIFIT2, hIFIT3, hIFIT5, rIFIT1 and rIFIT1B with tRNAs

The reported ability of IFIT5 to interact with tRNA (17) prompted us to characterize the tRNA-binding activity of other IFITs. First, we investigated association of hIFIT1, hIFIT2, hIFIT3, hIFIT5, rIFIT1 and rIFIT1B (at a concentration of 400 nM) with [^{32}P]-labeled Met-tRNA$_i^{Met}$, using EMSA (Figure 6A). The most efficient binding was observed for rIFIT1, rIFIT1B and hIFIT5, whereas binding of hIFIT1 was somewhat lower. In contrast, hIFIT2 showed very low affinity to Met-tRNA$_i^{Met}$, and no binding was detected in the case of hIFIT3. rIFIT1 and hIFIT5 bound to Met-tRNA$_i^{Met}$ as monomers, a small proportion of hIFIT1 formed dimers and higher order oligomers, whereas almost all rIFIT1B formed very large, slowly migrating oligomers. Interestingly, inclusion of eIF2 in a reaction mixture with Met-tRNA$_i^{Met}$ and rIFIT1B resulted in a specific supershift (Figure 6B), suggesting the possibility of simultaneous interaction of rIFIT1B and eIF2 with the same tRNA molecule, or of direct interaction between eIF2 and rIFIT1B.

To investigate whether association with tRNA influences binding of hIFIT1, rIFIT1 and rIFIT1B to the cap-proximal regions of cap0-mRNAs, competition experiments were performed. At a 10-fold excess over cap0-mRNA, tRNA$_i^{Met}$ reduced association of hIFIT1, rIFIT1, rIFIT1B with cap0-β-globin(G) mRNA to 38%, 25% and 21%, respectively (Figure 6C). Although the ability to inhibit IFIT/cap0-mRNA interaction was not restricted to tRNA$_i^{Met}$, other tested tRNAs (tRNA^{His}, tRNA^{Leu} and tRNA^{Lys}) showed lower activity, and when included at a 10-fold excess, reduced association of hIFIT1, rIFIT1, rIFIT1B with cap0-β-globin(G) mRNA by 40–44% (Figure 6D).

Investigation of the influence of hIFIT1 and rIFIT1B on 43S preinitiation complex formation

The ability to interfere with the assembly of 43 S preinitiation complexes has previously been suggested for hIFIT1 (30,31). We therefore decided to investigate the ribosomal binding activity of hIFIT1 and its influence on 43S complex formation using an *in vitro* reconstituted translation system. From among all tested IFITs, rIFIT1B and hIFIT1 were able to bind stably to 40S subunits and to remain associated with them during SDG centrifugation (Figure 7A). rIFIT1B bound more strongly than hIFIT1, but both were nevertheless present in substoichiometric amounts relative to 40S subunits, possibly due to the stringency of centrifugation. Interaction of both hIFIT1 and rIFIT1B with 40S subunits and Met-tRNA$_i^{Met}$ (Figure 6) prompted us to compare their influence on 43S complex formation. 43S complexes were assembled from 40S subunits, [^{35}S]Met-tRNA$_i^{Met}$ and eIFs 2, 3, 1 and 1 A, and analyzed by SDG centrifugation (Figure 7B). Neither hIFIT1 nor rIFIT1B affected 43S complex formation irrespective of whether [^{35}S]Met-tRNA$_i^{Met}$ (top panel), 40S subunits (middle panel), or [^{35}S]Met-tRNA$_i^{Met}$ and eIF2 (bottom panel) were preincubated with an excess of IFITs. Both IFITs also remained associated with 43S complexes during SDG centrifugation (Figure 7C).

Figure 5. Continued
hIFIT1 RNA binding cleft and the trajectory of the 5′-ppp in the hIFIT5 co-crystal structure is shown for comparison. Structure figures and alignments were generated using PyMol (Schrödinger). (**B**) Recombinant hIFIT1 mutants resolved by SDS-PAGE. (**C**) Interaction of hIFIT1 mutants (100 nM) with cap0-β-globin(G) mRNAs assayed by primer extension. Toe-prints induced by the IFIT1/mRNA interaction were quantified to determine the proportion of bound mRNA (%). (**D**) Inhibition by hIFIT1 mutants (100 nM) of 48S complex formation on cap0-β-globin(G) mRNA from 40S subunits, eIFs 2, 3, 1, 1A, 4A, 4B and 4F, and Met-tRNA$_i^{Met}$, assayed by toe-printing. Toe-prints corresponding to 48S complexes assembled in the presence of *wt* or mutant hIFIT1 were quantified relative to those observed in the absence of hIFIT1, which were defined as 100%.

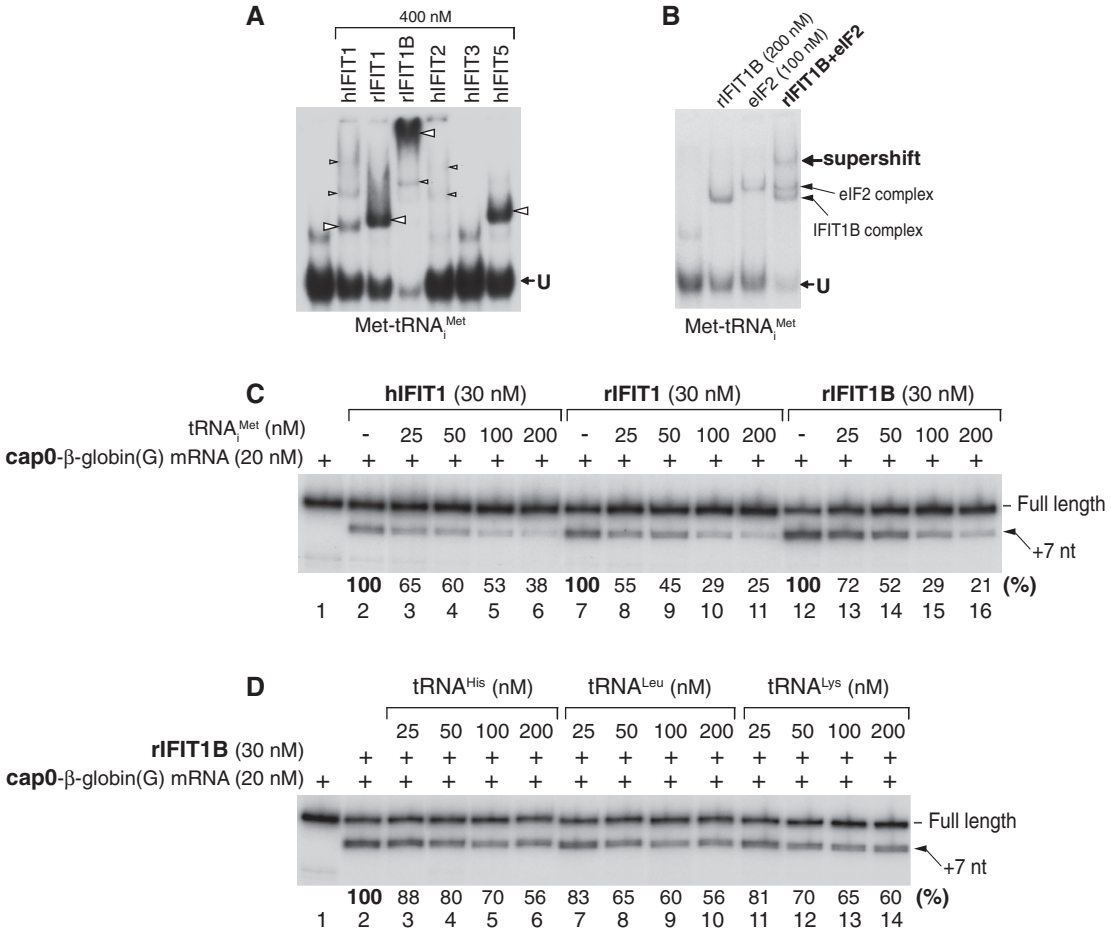

Figure 6. Interaction of hIFIT1, hIFIT2, hIFIT3, hIFIT5, rIFIT1 and rIFIT1B with tRNAs. (**A**) Interaction of hIFIT1, hIFIT2, hIFIT3, hIFIT5, rIFIT1 and rIFIT1B (400 nM) with [^{32}P]Met-tRNA$_i^{Met}$ assayed by EMSA. 'U' and 'B' indicate unbound and IFIT-bound Met-tRNA$_i^{Met}$, respectively. The positions of IFIT/Met-tRNA$_i^{Met}$ complexes in panel A are shown by arrowheads, with sizes corresponding to the amount of complex. (**B**) The ability of IFIT1B to form ternary complexes with eIF2 and Met-RNA$_i^{Met}$ assayed by EMSA. The positions of Met-tRNA$_i^{Met}$ in complex with IFIT1B and eIF2, as well as the supershift observed in the presence of both IFIT1B and eIF2 are indicated. (**C** and **D**) Inhibition of binding of hIFIT1, rIFIT1 and rIFIT1B (30 nM) to cap0-β-globin(G) mRNA (20 nM) by tRNA$_i^{Met}$, tRNA^{His}, tRNA^{Leu} and tRNA^{Lys} (25, 50, 100 and 200 nM) assayed by primer extension. Toe-prints induced by the IFIT/mRNA interaction are indicated.

DISCUSSION

Here we report that IFIT1 and IFIT1B (but not IFIT2, IFIT3 or IFIT5) bind specifically and with high affinity to the cap-proximal regions of cap0-mRNAs ($K_{1/2,app} \sim 9$ to 23 nM for β-globin cap0-mRNA). Interaction with mRNA occurs in a region of these proteins that is analogous to the narrow positively charged RNA-binding cleft in IFIT5 that accommodates 5′ppp-RNAs (16,18). Binding of IFIT1 and IFIT1B to cap0-mRNAs abrogates 48S complex formation in the *in vitro* reconstituted translation system.

The affinity of IFIT1 and IFIT1B enables them to outcompete eIF4E and eIF4F for binding to cap0-mRNA (Figure 3D and E). The ability of IFITs to outcompete individual eIF4E is consistent with its modest affinity to m^{7}GTP, for which K_d values in the majority of reports range from 140 to 260 nM, depending on the methodology and conditions used for the analysis (e.g. 48–50). The exact affinity for the cap of eIF4E as a subunit of eIF4F has not been determined, but it appears not to contribute significantly to the overall affinity of eIF4F for mRNA, because the apparent dissociation constants for binding of eIF4F to capped and uncapped mRNAs differ only slightly (18 ± 7 nM and 23 ± 7 nM for β-globin mRNA, respectively) (51). Although the overall affinity of eIF4F for mRNA is similar to that of IFIT1 and IFIT1B, IFITs strongly outcompete eIF4F for binding to cap0 mRNA. This suggests that the affinity of eIF4E bound to eIF4G within the eIF4F complex for the cap-terminal region of RNA is still substantially lower than that of IFIT1 and IFIT1B.

Interaction of cap-binding proteins with the cap commonly involves sandwiching of the methylated guanine base between two aromatic residues (e.g. W56/W102 in eIF4E, Y20/Y43 in the nuclear cap-binding protein CBC20, Y22/F180 in the vaccinia virus VP39 2′-*O*-methyltransferase and F104/H357 in the influenza virus polymerase subunit PB2) (52–56). However, sandwiching between aromatic and aliphatic residues has also been reported (e.g. W175/L206 in the scavenger decapping enzyme Dcps) (57). N7-methylation of guanine results in

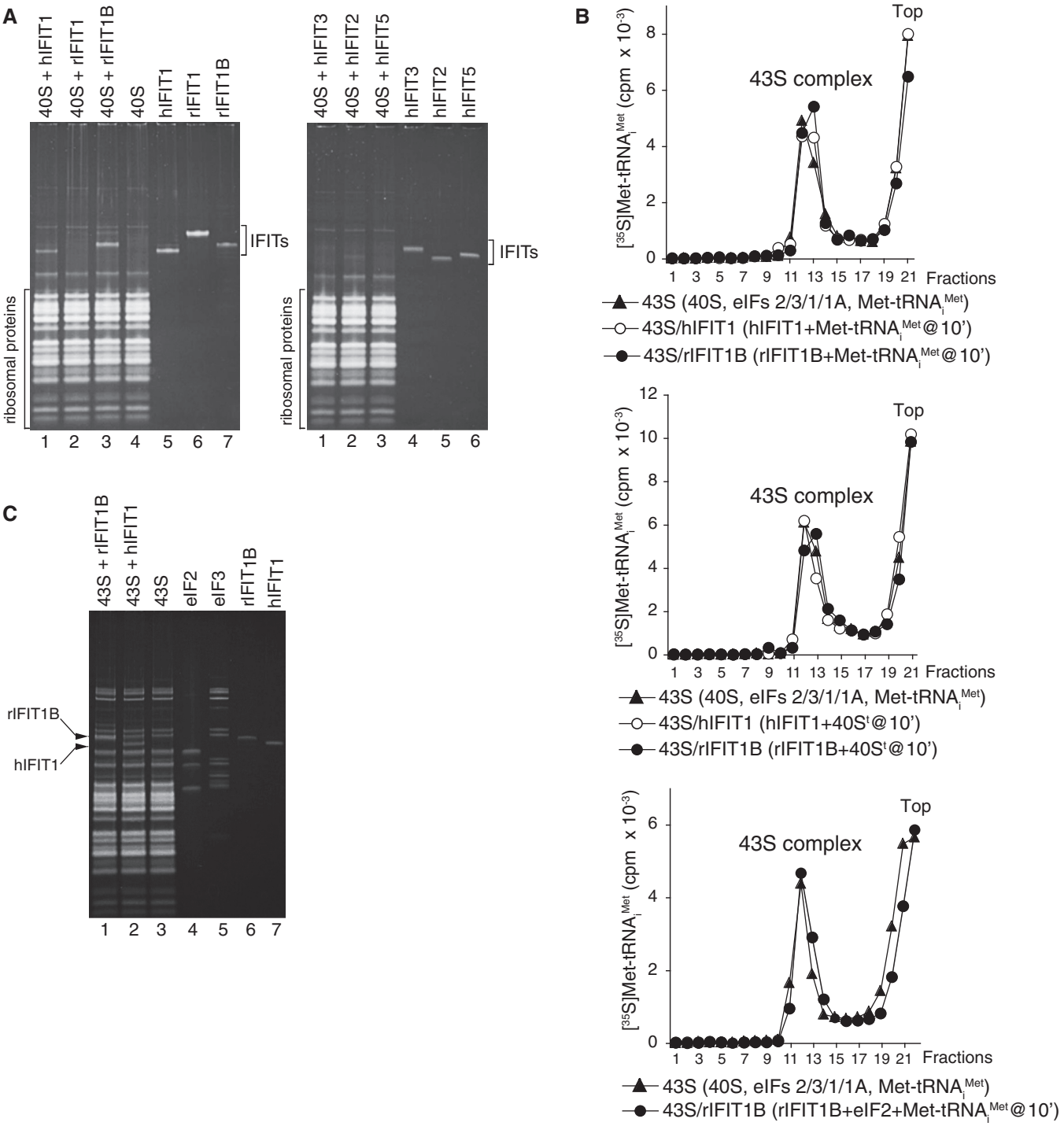

Figure 7. Association of hIFIT1, hIFIT2, hIFIT3, hIFIT5, rIFIT1 and rIFIT1B with 40S subunits and the influence of hIFIT1 and rIFIT1B on 43S preinitiation complex formation. (**A** and **C**) Association of hIFIT1, hIFIT2, hIFIT3, hIFIT5, rIFIT1 and rIFIT1B with (A) 40S subunits and (C) 43S preinitiation complexes assembled from 40S subunits, Met-tRNA$_i^{Met}$, eIF2, eIF3, eIF1 and eIF1A. Ribosomal complexes were separated by SDG centrifugation, and the presence of IFITs in ribosomal peak fractions was analyzed by SDS–PAGE followed by fluorescent SYPRO staining. (**B**) Influence of hIFIT1 and rIFIT1B on 43S complex assembly from 40S subunits, [^{35}S]Met-tRNA$_i^{Met}$, eIF2, eIF3, eIF1 and eIF1A, depending on preincubation of IFITs with either Met-tRNA$_i^{Met}$ (top panel), 40S subunits (middle panel) or eIF2 and Met-tRNA$_i^{Met}$ (bottom panel). Ribosomal complexes were separated by SDG centrifugation followed by scintillation counting of [^{35}S]Met-tRNA$_i^{Met}$. Sedimentation was from right to left.

delocalization of the positive charge on the base in its cationic form, which enhances the interactions with the π-electrons of the stacked aromatic rings (58,59), accounting for the specificity of binding to the N7-methylated cap over its unmethylated counterpart. In most instances, the enhancement of binding by N7-methylation is strong, amounting to 2 to 3 orders of magnitude for eIF4E (60), eIF4E3 (49) and CBC20 (61). The putative pocket in

IFIT1 that could accommodate the m^7G moiety includes several aromatic residues, of which W147 and Y218 were critical for binding of IFIT1 to cap0-mRNA (Figure 5), and could therefore be directly involved in cap recognition. However, any speculation concerning potential stacking interactions involving these residues is premature because considerable conformational change occurs in IFIT5 as a consequence of its binding to 5′ppp-RNA (16), and might similarly accompany binding of cap0-RNA to IFIT1. Although N7-methylation enhanced the affinity of IFIT1 and IFIT1B for cap0-RNA by only ~3.5- and ~10-fold, respectively, these modest increases are not unprecedented, as a similar 5-fold enhancement was reported for the influenza PB2 polymerase subunit (56). Low dependence on N7-methylation suggests that interactions other than with m^7G contribute significantly to the affinity of IFIT1 and IFIT1B to cap0-RNAs. The affinity of several cap-binding proteins to capped mRNA is known to be enhanced by cap-proximal nucleotides. Thus, binding of CBC20 to the cap is enhanced by the first 2 nt, and influenza PB2 requires at least 4 nt for efficient interaction and binds even more strongly if 9 nt are present (62). Based on the arrest of RT at positions +6−8 nt from the 5′-end on the IFIT1/cap0-RNA and IFIT1B/cap0-RNA complexes, the interaction of IFIT1 and IFIT1B with mRNA also involves at least 4–5 nt, which is in turn consistent with the number of nucleotides that are observed to interact with IFIT5 in the co-crystal structure (16).

The interaction of IFIT1 with RNA was abrogated by 2′-*O*-methylation: in primer extension inhibition experiments, no binding was observed for human and rabbit IFIT1 to cap1-mRNA. rIFIT1B, on the other hand, retained the ability to bind to cap1-RNA, but with an affinity ($K_{1/2,app} \sim 450$ nM) that was more than one order of magnitude lower than for cap0-RNA ($K_{1/2,app} \sim 9$ nM). If the paths for the first 4 nt of RNA bound to IFIT1 and IFIT1B are similar to that of 5′ppp-RNA bound to IFIT5, then a clash of the 2′-*O*-methyl group of cap1-RNA with R187 of IFIT1 (R186 in IFIT5) might be expected. Stable binding was also observed between IFIT5 and 5′ppp-mRNA, with an affinity ($K_{1/2,app} \sim 400$ nM) that is comparable to that determined previously by EMSA ($K_d = 250$–500 nM) (16). IFIT1, on the other hand, did not stably interact with 5′ppp-mRNA, even though moderate-affinity binding of IFIT1 to such RNAs was detected by surface plasmon resonance ($K_d \sim 240$ nM) (10). Although this discrepancy could be explained by potential displacement of IFIT1 by RT during primer extension, the fact that in contrast to IFIT5, IFIT1 did not inhibit 48S complex formation on 5′ppp-mRNA suggests that its affinity to 5′ppp-mRNA is lower than that of IFIT5. Importantly, although detected, interactions of IFIT1B and IFIT5 with cap1- and 5′ppp-mRNAs were substantially weaker than specific interactions of IFIT1 and IFIT1B with cap0-mRNAs.

Similarly to IFIT5 (17), IFIT1 and IFIT1B also bound to initiator tRNA. In IFIT5, the tRNA-binding surface was assigned to an area in close proximity to the entrance of the 5′ppp-RNA-binding pocket (17; Figure 5A), and tRNA binding to this site on hIFIT5, or to a homologous position on hIFIT1, would be expected to occlude the narrow ssRNA binding cleft. The observed competition between initiator tRNA and cap0-mRNA for binding to IFIT1 and IFIT1B is consistent with this model. Although initiator tRNA was the best competitor, the fact that other tested elongator tRNAs were also able to interfere with the binding of IFITs to cap0-mRNA is indicative of the low specificity of IFIT/tRNA binding. hIFIT1 and rIFIT1B were also able to interact with 40S subunits, which could potentially involve a non-specific interaction between exposed elements of 18S rRNA and the tRNA-binding regions of these IFITs. In any case, this interaction is not very strong since both IFITs were bound to 40S subunits in sub-stoichiometric amounts. Importantly, despite their interactions with initiator tRNA and the 40S subunit, IFIT1 and IFIT1B did not interfere with the assembly of 43S preinitiation complexes, as suggested for human IFIT1 (30,31).

Although the various IFITs could bind tRNA and 40S subunits, the activity of individual IFITs in inhibiting 48S complex formation on a specific mRNA was determined by their ability to interact specifically with its 5′-terminal region. The strongest inhibition was mediated by IFIT1 and IFIT1B on cap0-mRNA, followed by IFIT1B-mediated inhibition on cap1-mRNA, and then by inhibition on 5′ppp-mRNA by IFIT5. Other combinations of IFITs and mRNAs did not exhibit any inhibition. Taking the level of inhibition into account, suppression of initiation on cap0-mRNAs by IFIT1 and IFIT1B is likely to be physiologically the most important. The abundance of IFIT1 and IFIT1B and their ability to competitively inhibit binding of eIF4F to cap0-mRNAs form the basis of a mechanism for regulation of translation of any mRNA that has a 5′-terminal cap0. The lack of specificity of the IFIT1(IFIT1B)/cap0-mRNA interaction differentiates this mechanism from others that sequester the cap of specific mRNAs to prevent their functional interaction with eIF4F, such as the enhanced binding of the *Drosophila* 4 E-homologous protein (d4EHP) to the 5′-terminal cap of *Caudal* mRNA by Bicoid (which binds d4EHP and the 3′UTR of *Caudal* mRNA) (63), and of eIF4E to the cap of *Oskar* mRNA by Cup (which interacts with eIF4E and the *Oskar* 3′UTR-binding protein Bruno) (e.g. 64).

Expression of IFIT1 is strongly up-regulated in response to viral infection by IFN-dependent and -independent mechanisms (8,65), and IFIT1-mediated translational regulation likely primarily targets viral mRNAs. However, IFIT1 may also have other targets, since it is constitutively expressed in various cells including human skin fibroblasts (66) and some sarcoma cell lines (67), over-expressed in $CD34^+$ cells of patients with hematopoetic malignancies (68) and influences the radiation sensitivity of early-stage breast cancer (69). IFIT1B is thought not to be expressed in an IFN-dependent manner (11), but as neither the cell types in which it occurs nor the circumstances that induce its expression are known, speculation about its physiological importance in translational control mechanisms is premature. However, it clearly has the potential to act as a more

wide-ranging inhibitor of translation than IFIT1, because of its ability to bind to cap1-mRNAs.

Which mRNAs are potential regulatory targets for the cap0-binding activity of IFIT1 and IFIT1B? Viruses such as Sindbis virus do not encode a 2′-*O*-methyltransferase, and their cap0-mRNAs are therefore strong candidates for inhibition by IFIT1 and IFIT1B. Consistently, Sindbis virus replication was impaired by over-expression of IFIT1 and enhanced by its siRNA-mediated silencing (21). Moreover, the absence of IFIT1 in *Ifit*$^{-/-}$ mice and murine embryonic fibroblasts and macrophages enhanced replication of 2′-*O*-methylation-defective mutant forms of human coronavirus 229 E and mouse hepatitis virus (family *Coronaviridae*), poxvirus (family *Poxviridae*), West Nile virus and Japanese encephalitis virus (family *Flaviviridae*), which are normally very sensitive to innate immune responses (22,35,70–72). For most viruses, the enzymes that catalyze N7-methylation and 2′-*O*-methylation of viral mRNA are part of either a multi-domain protein or a 'cap assembly line', and the reactions are consequently tightly coupled (2). However, in some instances they may be temporally separated, for example if they are catalyzed by enzymes that function in a defined order (such as the SARS-coronavirus nsp14 guanine-N7-methyltransferase and nsp10/nsp16 nucleoside-2′-*O*-methyltransferase) (73). In such cases, it would hypothetically be possible for IFIT1 to sequester viral mRNAs after synthesis of cap0 but before completion of cap1 formation.

Inhibition of translation of cellular mRNAs by IFIT1 would also require the presence of 'cap0' at their 5′-termini. Formation of cap0 is a co-transcriptional process, and mRNAs that lack the N7-methyl moiety are recognized as being incorrectly capped and are degraded (74), whereas correctly capped mRNAs are sequentially methylated at the 2′-hydroxyl position of the first and second transcribed riboses by nuclear and cytoplasmic cap-specific 2′-*O* nucleoside RNA methytransferases, respectively, yielding cap1 and cap2 structures (e.g. 75). If there were a failure of capping to proceed beyond cap0 formation, the resulting mRNAs would be susceptible to regulation by IFIT1, and it is conceivable that IFIT1 might function as part of a complex that detects and degrades incompletely capped mRNAs. However, cap0-mRNAs appear to be stable, at least in some circumstances, since stored maternal mRNA in *Xenopus* oocytes undergo maturation-dependent 2′-*O*-methylation, which is thought to contribute to their translational activation (76–78). Temporal separation of cap formation and 2′-*O*-methylation could thus occur in a regulated manner. The 2′-*O*-methylation to form cap1 has only a modest effect on ribosomal recruitment *per se* (79), so that its suggested role in translational activation could potentially reflect relief from IFIT-mediated repression rather than direct enhancement. Another circumstance that leads to the accumulation of uncapped mRNAs involves the regulated decapping and partial removal of the 5′UTR from mRNAs in the cytoplasm. It has recently been determined that these mRNAs can undergo cytoplasmic recapping by an as-yet unidentified enzyme. This process would yield mRNAs lacking 2′-*O*-methylation, which would thus be susceptible to IFIT1-mediated sequestration (80,81).

SUPPLEMENTARY DATA

Supplementary Data are available at NAR Online.

ACKNOWLEDGEMENTS

We thank Kathleen Collins, George Katibah, Yingfang Liu, Andreas Pichlmair and Katherine Borden for their gifts of hIFIT1, hIFIT2, hIFIT3, hIFIT5 and eIF4E expression vectors. M.S. and O.S. initiated the project and made equal contributions.

FUNDING

National Institutes of Health (NIH) [GM59660 to T.V.P. and AI51340 to C.U.T.H.]. Funding for open access charge: NIH.

Conflict of interest statement. None declared.

REFERENCES

1. Goubau,D., Deddouche,S. and Reis e Sousa,C. (2013) Cytosolic sensing of viruses. *Immunity*, **38**, 855–869.
2. Decroly,E., Ferron,F., Lescar,J. and Canard,B. (2011) Conventional and unconventional mechanisms for capping viral mRNA. *Nat. Rev. Microbiol.*, **10**, 51–65.
3. Young,R.J. and Content,J. (1971) 5′-terminus of influenza virus RNA. *Nat. New Biol.*, **230**, 140–142.
4. Dubin,D.T. and Stollar,V. (1975) Methylation of Sindbis virus '26S' messenger RNA. *Biochem. Biophys. Res. Commun.*, **66**, 1373–1379.
5. Hefti,E., Bishop,D.H.L., Dubin,D.T. and Stollar,V. (1976) 5′ nucleotide sequence of sindbis viral RNA. *J. Virol.*, **17**, 149–159.
6. Diamond,M.S. and Farzan,M. (2013) The broad-spectrum antiviral functions of IFIT and IFITM proteins. *Nat. Rev. Immunol.*, **13**, 46–57.
7. deVeer,M.J., Holko,M., Frevel,M., Walker,E., Der,S., Paranjape,J.M., Silverman,R.H. and Williams,B.R. (2001) Functional classification of interferon-stimulated genes identified using microarrays. *J. Leukoc. Biol.*, **69**, 912–920.
8. Der,S.D., Zhou,A., Williams,B.R.G. and Silverman,R.H. (1998) Identification of genes differentially regulated by interferon α, β, or γ using oligonucleotide arrays. *Proc. Natl Acad. Sci. USA*, **95**, 15623–15628.
9. Indraccolo,S., Pfeffer,U., Minuzzo,S., Esposito,G., Roni,V., Mandruzzato,S., Ferrari,N., Anfosso,L., Dell'Eva,R., Noonan,D.M. *et al.* (2007) Identification of genes selectively regulated by IFNs in endothelial cells. *J. Immunol.*, **178**, 1122–1135.
10. Pichlmair,A., Lassnig,C., Eberle,C.A., Górna,M.W., Baumann,C.L., Burkard,T.R., Bürckstümmer,T., Stefanovic,A., Krieger,S., Bennett,K.L. *et al.* (2011) IFIT1 is an antiviral protein that recognizes 5′-triphosphate RNA. *Nat. Immunol.*, **12**, 624–630.
11. Fensterl,V. and Sen,G.C. (2011) The ISG56/IFIT1 gene family. *J. Interferon Cytokine Res.*, **31**, 71–78.
12. Liu,Y., Zhang,Y.B., Liu,T.K. and Gui,J.F. (2013) Lineage-specific expansion of IFIT gene family: an insight into coevolution with IFN gene family. *PLoS One*, **8**, e66859.
13. Zhou,X., Michal,J.J., Zhang,L., Ding,B., Lunney,J.K., Liu,B. and Jiang,Z. (2013) Interferon induced IFIT family genes in host antiviral defense. *Int. J. Biol. Sci.*, **9**, 200–208.
14. Zeytuni,N. and Zarivach,R. (2012) Structural and functional discussion of the tetra-trico-peptide repeat, a protein interaction module. *Structure*, **20**, 397–405.

15. Yang,Z., Liang,H., Zhou,Q., Li,Y., Chen,H., Ye,W., Chen,D., Fleming,J., Shu,H. and Liu,Y. (2012) Crystal structure of ISG54 reveals a novel RNA binding structure and potential functional mechanisms. *Cell Res.*, **22**, 1328–1338.
16. Abbas,Y.M., Pichlmair,A., Górna,M.W., Superti-Furga,G. and Nagar,B. (2013) Structural basis for viral 5′-PPP-RNA recognition by human IFIT proteins. *Nature*, **494**, 60–64.
17. Katibah,G.E., Lee,H.J., Huizar,J.P., Vogan,J.M., Alber,T. and Collins,K. (2013) tRNA binding, structure, and localization of the human interferon-induced protein IFIT5. *Mol. Cell*, **49**, 743–750.
18. Feng,F., Yuan,L., Wang,Y.E., Crowley,C., Lv,Z., Li,J., Liu,Y., Cheng,G., Zeng,S. and Liang,H. (2013) Crystal structure and nucleotide selectivity of human IFIT5/ISG58. *Cell Res.*, **23**, 1055–1058.
19. Terenzi,F., Hui,D.J., Merrick,W.C. and Sen,G.C. (2006) Distinct induction patterns and functions of two closely related interferon-inducible human genes, ISG54 and ISG56. *J. Biol. Chem.*, **281**, 34064–34071.
20. Wacher,C., Müller,M., Hofer,M.J., Getts,D.R., Zabaras,R., Ousman,S.S., Terenzi,F., Sen,G.C., King,N.J. and Campbell,I.L. (2007) Coordinated regulation and widespread cellular expression of interferon-stimulated genes (ISG) ISG-49, ISG-54, and ISG-56 in the central nervous system after infection with distinct viruses. *J. Virol.*, **81**, 860–871.
21. Zhang,Y., Burke,C.W., Ryman,K.D. and Klimstra,W.B. (2007) Identification and characterization of interferon-induced proteins that inhibit alphavirus replication. *J. Virol.*, **81**, 11246–11255.
22. Daffis,S., Szretter,K.J., Schriewer,J., Li,J., Youn,S., Errett,J., Lin,T.Y., Schneller,S., Zust,R., Dong,H. *et al.* (2010) 2′-O methylation of the viral mRNA cap evades host restriction by IFIT family members. *Nature*, **468**, 452–456.
23. Fensterl,V., Wetzel,J.L., Ramachandran,S., Ogino,T., Stohlman,S.A., Bergmann,C.C., Diamond,M.S., Virgin,H.W. and Sen,G.C. (2012) Interferon-induced Ifit2/ISG54 protects mice from lethal VSV neuropathogenesis. *PLoS Pathog.*, **8**, e1002712.
24. Liu,X.Y., Chen,W., Wei,B., Shan,Y.F. and Wang,C. (2011) IFN-induced TPR protein IFIT3 potentiates antiviral signaling by bridging MAVS and TBK1. *J. Immunol.*, **187**, 2559–2568.
25. Zhang,B., Liu,X., Chen,W. and Chen,L. (2013) IFIT5 potentiates anti-viral response through enhancing innate immune signaling pathways. *Acta Biochim. Biophys. Sin. (Shanghai)*, **45**, 867–874.
26. Li,Y., Li,C., Xue,P., Zhong,B., Mao,A.P., Ran,Y., Chen,H., Wang,Y.Y., Yang,F. and Shu,H.B. (2009) ISG56 is a negative-feedback regulator of virus-triggered signaling and cellular antiviral response. *Proc. Natl Acad. Sci. USA.*, **106**, 7945–7950.
27. Stawowczyk,M., Van Scoy,S., Kumar,K.P. and Reich,N.C. (2011) The interferon stimulated gene 54 promotes apoptosis. *J. Biol. Chem.*, **286**, 7257–7266.
28. Reich,N.C. (2013) A death-promoting role for ISG54/IFIT2. *J. Interferon Cytokine Res.*, **33**, 199–205.
29. Guo,J., Hui,D.J., Merrick,W.C. and Sen,G.C. (2000) A new pathway of translational regulation mediated by eukaryotic initiation factor 3. *EMBO J.*, **19**, 6891–6899.
30. Hui,D.J., Bhasker,C.R., Merrick,W.C. and Sen,G.C. (2003) Viral stress-inducible protein p56 inhibits translation by blocking the interaction of eIF3 with the ternary complex eIF2.GTP.Met-tRNAi. *J. Biol. Chem.*, **278**, 39477–39482.
31. Hui,D.J., Terenzi,F., Merrick,W.C. and Sen,G.C. (2005) Mouse p56 blocks a distinct function of eukaryotic initiation factor 3 in translation initiation. *J. Biol. Chem.*, **280**, 3433–3440.
32. Jackson,R.J., Hellen,C.U. and Pestova,T.V. (2010) The mechanism of eukaryotic translation initiation and principles of its regulation. *Nat. Rev. Mol. Cell. Biol.*, **11**, 113–127.
33. Hashem,Y., des Georges,A., Dhote,V., Langlois,R., Liao,H.Y., Grassucci,R.A., Hellen,C.U., Pestova,T.V. and Frank,J. (2013) Structure of the mammalian ribosomal 43S preinitiation complex bound to the scanning factor DHX29. *Cell*, **153**, 1108–1119.
34. Hogg,J.R. and Collins,K. (2007) Human Y5 RNA specializes a Ro ribonucleoprotein for 5S ribosomal RNA quality control. *Genes Dev.*, **21**, 3067–3072.
35. Kimura,T., Katoh,H., Kayama,H., Saiga,H., Okuyama,M., Okamoto,T., Umemoto,E., Matsuura,Y., Yamamoto,M. and Takeda,K. (2013) Ifit1 inhibits Japanese encephalitis virus teplication through binding to 5′ capped 2′-O unmethylated RNA. *J. Virol.*, **87**, 9997–10003.
36. Habjan,M., Hubel,P., Lacerda,L., Benda,C., Holze,C., Eberl,C.H., Mann,A., Kindler,E., Gil-Cruz,C., Ziebuhr,J. *et al.* (2013) Sequestration by IFIT1 impairs translation of 2′O-unmethylated capped RNA. *PLoS Pathog.*, **9**, e1003663.
37. Pestova,T.V., Borukhov,S.I. and Hellen,C.U. (1998) Eukaryotic ribosomes require initiation factors 1 and 1A to locate initiation codons. *Nature*, **394**, 854–859.
38. Pestova,T.V., Hellen,C.U. and Shatsky,I.N. (1996) Canonical eukaryotic initiation factors determine initiation of translation by internal ribosomal entry. *Mol. Cell. Biol.*, **16**, 6859–6869.
39. Volpon,L., Osborne,M.J., Topisirovic,I., Siddiqui,N. and Borden,K.L. (2006) Cap-free structure of eIF4E suggests a basis for conformational regulation by its ligands. *EMBO J.*, **25**, 5138–5149.
40. Lomakin,I.B., Shirokikh,N.E., Yusupov,M.M., Hellen,C.U. and Pestova,T.V. (2006) The fidelity of translation initiation: reciprocal activities of eIF1, IF3 and YciH. *EMBO J.*, **25**, 196–210.
41. Skabkin,M.A., Skabkina,O.V., Hellen,C.U. and Pestova,T.V. (2013) Reinitiation and other unconventional posttermination events during eukaryotic translation. *Mol. Cell*, **51**, 249–264.
42. Pestova,T.V. and Hellen,C.U. (2001) Preparation and activity of synthetic unmodified mammalian tRNAi(Met) in initiation of translation in vitro. *RNA*, **7**, 1496–1505.
43. Pisarev,A.V., Hellen,C.U. and Pestova,T.V. (2007) Recycling of eukaryotic posttermination ribosomal complexes. *Cell*, **131**, 286–299.
44. Hagedorn,C.H., Spivak-Kroizman,T., Friedland,D.E., Goss,D.J. and Xie,Y. (1997) Expression of functional eIF-4Ehuman: purification, detailed characterization, and its use in isolating eIF-4E binding proteins. *Protein Expr Purif.*, **9**, 53–60.
45. Pisarev,A.V., Unbehaun,A., Hellen,C.U. and Pestova,T.V. (2007) Assembly and analysis of eukaryotic translation initiation complexes. *Methods Enzymol.*, **430**, 147–177.
46. Sweeney,T.R., Cisnetto,V., Bose,D., Bailey,M., Wilson,J.R., Zhang,X., Belsham,G.J. and Curry,S. (2010) Foot-and-mouth disease virus 2C is a hexameric AAA+ protein with a coordinated ATP hydrolysis mechanism. *J. Biol. Chem.*, **285**, 24347–24359.
47. Pisarev,A.V., Skabkin,M.A., Pisareva,V.P., Skabkina,O.V., Rakotondrofara,A.M., Hentze,M.W., Hellen,C.U.T. and Pestova,T.V. (2010) The role of ABCE1 in eukaryotic posttermination ribosomal recycling. *Mol. Cell*, **37**, 196–210.
48. Brown,C.J., McNae,I., Fischer,P.M. and Walkinshaw,M.D. (2007) Crystallographic and mass spectrometric characterisation of eIF4E with N7-alkylated cap derivatives. *J. Mol. Biol.*, **372**, 7–15.
49. Osborne,M.J., Volpon,L., Kornblatt,J.A., Culjkovic-Kraljacic,B., Baguet,A. and Borden,K.L. (2013) eIF4E3 acts as a tumor suppressor by utilizing an atypical mode of methyl-7-guanosine cap recognition. *Proc. Natl Acad. Sci. USA.*, **110**, 3877–3882.
50. Scheper,G.C., van Kollenburg,B., Hu,J., Luo,Y., Goss,D.J. and Proud,C.G. (2002) Phosphorylation of eukaryotic initiation factor 4E markedly reduces its affinity for capped mRNA. *J. Biol. Chem.*, **277**, 3303–3309.
51. Kaye,N.M., Emmett,K.J., Merrick,W.C. and Jankowsky,E. (2009) Intrinsic RNA binding by the eukaryotic initiation factor 4F depends on a minimal RNA length but not on the m7G cap. *J. Biol. Chem.*, **284**, 17742–17750.
52. Matsuo,H., Li,H., McGuire,A.M., Fletcher,C.M., Gingras,A.C., Sonenberg,N. and Wagner,G. (1997) Structure of translation factor eIF4E bound to m7GDP and interaction with 4E-binding protein. *Nat. Struct. Biol.*, **4**, 717–724.
53. Marcotrigiano,J., Gingras,A.C., Sonenberg,N. and Burley,S.K. (1997) Cocrystal structure of the messenger RNA 5′ cap-binding protein (eIF4E) bound to 7-methyl-GDP. *Cell*, **89**, 951–961.
54. Hodel,A.E., Gershon,P.D., Shi,X., Wang,S.M. and Quiocho,F.A. (1997) Specific protein recognition of an mRNA cap through its alkylated base. *Nat. Struct. Biol.*, **4**, 350–354.
55. Mazza,C., Segref,A., Mattaj,I.W. and Cusacks,S. (2002) Large-scale induced fit recognition of an m(7)GpppG cap analogue by the human nuclear cap-binding complex. *EMBO J.*, **21**, 5548–5557.

56. Guilligay,D., Tarendeau,F., Resa-Infante,P., Coloma,R., Crepin,T., Sehr,P., Lewis,J., Ruigrok,R.W., Ortin,J., Hart,D.J. *et al.* (2008) The structural basis for cap binding by influenza virus polymerase subunit PB2. *Nat. Struct. Mol. Biol.*, **15**, 500–506.
57. Gu,M., Fabrega,C., Liu,S.W., Liu,H., Kiledjian,M. and Lima,C.D. (2004) Insights into the structure, mechanism, and regulation of scavenger mRNA decapping activity. *Mol. Cell*, **14**, 67–80.
58. Hu,G., Gershon,P.D., Hodel,A.E. and Quiocho,F.A. (1999) mRNA cap recognition: dominant role of enhanced stacking interactions between methylated bases and protein aromatic side chains. *Proc. Natl Acad. Sci. USA*, **96**, 7149–7154.
59. Quiocho,F.A., Hu,G. and Gershon,P.D. (2000) Structural basis of mRNA cap recognition by proteins. *Curr. Opin. Struct. Biol.*, **10**, 78–86.
60. Niedzwiecka,A., Marcotrigiano,J., Stepinski,J., Jankowska-Anyszka,M., Wyslouch-Cieszynska,A., Dadlez,M., Gingras,A.C., Mak,P., Darzynkiewicz,E., Sonenberg,N. *et al.* (2002) Biophysical studies of eIF4E cap-binding protein: recognition of mRNA 5′ cap structure and synthetic fragments of eIF4G and 4E-BP1 proteins. *J. Mol. Biol.*, **319**, 615–635.
61. Worch,R., Niedzwiecka,A., Stepinski,J., Mazza,C., Jankowska-Anyszka,M., Darzynkiewicz,E., Cusack,S. and Stolarski,R. (2005) Specificity of recognition of mRNA 5′ cap by human nuclear cap-binding complex. *RNA*, **11**, 1355–1363.
62. Chung,T.D., Cianci,C., Hagen,M., Terry,B., Matthews,J.T., Krystal,M. and Colonno,R.J. (1994) Biochemical studies on capped RNA primers identify a class of oligonucleotide inhibitors of the influenza virus RNA polymerase. *Proc. Natl Acad. Sci. USA*, **91**, 2372–2376.
63. Cho,P.F., Poulin,F., Cho-Park,Y.A., Cho-Park,I.B., Chicoine,J.D., Lasko,P. and Sonenberg,N. (2005) A new paradigm for translational control: inhibition via 5′-3′ mRNA tethering by Bicoid and the eIF4E cognate 4EHP. *Cell*, **121**, 411–423.
64. Nakamura,A., Sato,K. and Hanyu-Nakamura,K. (2004) Drosophila cup is an eIF4E binding protein that associates with Bruno and regulates oskar mRNA translation in oogenesis. *Dev. Cell*, **6**, 69–78.
65. Grandvaux,N., Servant,M.J., tenOever,B., Sen,G.C., Balachandran,S., Barber,G.N., Lin,R. and Hiscott,J. (2002) Transcriptional profiling of interferon regulatory factor 3 target genes: direct involvement in the regulation of interferon-stimulated genes. *J. Virol.*, **76**, 5532–5539.
66. Moll,H.P., Maier,T., Zommer,A., Lavoie,T. and Brostjan,C. (2011) The differential activity of interferon-α subtypes is consistent among distinct target genes and cell types. *Cytokine*, **53**, 52–59.
67. Berchtold,S., Lampe,J., Weiland,T., Smirnow,I., Schleicher,S., Handgretinger,R., Kopp,H.G., Reiser,J., Stubenrauch,F., Mayer,N. *et al.* (2013) Innate immune defense defines susceptibility of sarcoma cells to measles vaccine virus-based oncolysis. *J. Virol.*, **87**, 3484–3501.
68. Pellagatti,A., Cazzola,M., Giagounidis,A.A., Malcovati,L., Porta,M.G., Killick,S., Campbell,L.J., Wang,L., Langford,C.F., Fidler,C. *et al.* (2006) Gene expression profiles of CD34+ cells in myelodysplastic syndromes: involvement of interferon-stimulated genes and correlation to FAB subtype and karyotype. *Blood*, **108**, 337–345.
69. Danish,H.H., Goyal,S., Taunk,N.K., Wu,H., Moran,M.S. and Haffty,B.G. (2013) Interferon-induced protein with tetratricopeptide repeats 1 (IFIT1) as a prognostic marker for local control in T1-2 N0 breast cancer treated with breast-conserving surgery and radiation therapy (BCS + RT). *Breast J.*, **19**, 231–239.
70. Züst,R., Cervantes-Barragan,L., Habjan,M., Maier,R., Neuman,B.W., Ziebuhr,J., Szretter,K.J., Baker,S.C., Barchet,W., Diamond,M.S. *et al.* (2011) Ribose 2′-O-methylation provides a molecular signature for the distinction of self and non-self mRNA dependent on the RNA sensor MDA5. *Nat. Immunol.*, **12**, 137–143.
71. Züst,R., Dong,H., Li,X.F., Chang,D.C., Zhang,B., Balakrishnan,T., Toh,Y.X., Jiang,T., Li,S.H., Deng,Y.Q. *et al.* (2013) Rational design of a live attenuated dengue vaccine: 2′-o-methyltransferase mutants are highly attenuated and immunogenic in mice and macaques. *PLoS Pathog.*, **9**, e1003521.
72. Szretter,K.J., Daniels,B.P., Cho,H., Gainey,M.D., Yokoyama,W.M., Gale,M. Jr, Virgin,H.W., Klein,R.S., Sen,G.C. and Diamond,M.S. (2012) 2′-O methylation of the viral mRNA cap by West Nile virus evades IFIT1-dependent and -independent mechanisms of host restriction *in vivo*. *PLoS Pathog.*, **8**, e1002698.
73. Bouvet,M., Debarnot,C., Imbert,I., Selisko,B., Snijder,E.J., Canard,B. and Decroly,E. (2010) In vitro reconstitution of SARS-coronavirus mRNA cap methylation. *PLoS Pathog.*, **6**, e1000863.
74. Jiao,X., Xiang,S., Oh,C., Martin,C.E., Tong,L. and Kiledjian,M. (2010) Identification of a quality-control mechanism for mRNA 5′-end capping. *Nature*, **467**, 608–611.
75. Bélanger,F., Stepinski,J., Darzynkiewicz,E. and Pelletier,J. (2010) Characterization of hMTr1, a human cap1 2′-O-ribose methyltransferase. *J. Biol. Chem.*, **285**, 33037–33044.
76. Kuge,H., Brownlee,G.G., Gershon,P.D. and Richter,J.D. (1998) Cap ribose methylation of c-mos mRNA stimulates translation and oocyte maturation in Xenopus laevis. *Nucleic Acids Res.*, **26**, 3208–3214.
77. Kuge,H. and Richter,J.D. (1995) Cytoplasmic 3′ poly(A) addition induces 5′ cap ribose methylation: implications for translational control of maternal mRNA. *EMBO J.*, **14**, 6301–6310.
78. Gillian-Daniel,D.L., Gray,N.K., Aström,J., Barkoff,A. and Wickens,M. (1998) Modifications of the 5′ cap of mRNAs during Xenopus oocyte maturation: independence from changes in poly(A) length and impact on translation. *Mol. Cell. Biol.*, **18**, 6152–6163.
79. Muthukrishnan,S., Moss,B., Cooper,J.A. and Maxwell,E.S. (1978) Influence of 5′-terminal cap structure on the initiation of translation of vaccinia virus mRNA. *J. Biol. Chem.*, **253**, 1710–1715.
80. Schoenberg,D.R. and Maquat,L.E. (2009) Re-capping the message. *Trends Biochem. Sci.*, **34**, 435–442.
81. Mukherjee,C., Patil,D.P., Kennedy,B.A., Bakthavachalu,B., Bundschuh,R. and Schoenberg,D.R. (2012) Identification of cytoplasmic capping targets reveals a role for cap homeostasis in translation and mRNA stability. *Cell Rep.*, **2**, 674–684.